Schneider and Bláha *Environ Sci Eur* (2020) 32:94
https://doi.org/10.1186/s12302-020-00371-0

Environmental Sciences Europe

REVIEW Open Access

Advanced oxidation processes for the removal of cyanobacterial toxins from drinking water

Marcel Schneider* and Luděk Bláha

Abstract

Drinking water production faces many different challenges with one of them being naturally produced cyanobacterial toxins. Since pollutants become more abundant and persistent today, conventional water treatment is often no longer sufficient to provide adequate removal. Among other emerging technologies, advanced oxidation processes (AOPs) have a great potential to appropriately tackle this issue. This review addresses the economic and health risks posed by cyanotoxins and discusses their removal from drinking water by AOPs. The current state of knowledge on AOPs and their application for cyanotoxin degradation is synthesized to provide an overview on available techniques and effects of water quality, toxin- and technique-specific parameters on their degradation efficacy. The different AOPs are compared based on their efficiency and applicability, considering economic, practical and environmental aspects and their potential to generate toxic disinfection byproducts. For future research, more relevant studies to include the degradation of less-explored cyanotoxins, toxin mixtures in actual surface water, assessment of residual toxicity and scale-up are recommended. Since actual surface water most likely contains more than just cyanotoxins, a multi-barrier approach consisting of a series of different physical, biological and chemical—especially oxidative—treatment steps is inevitable to ensure safe and high-quality drinking water.

Keywords: AOP, Cyanotoxin, Cylindrospermopsin, Fenton oxidation, Hydroxyl radical, Microcystin, Ozone, Sulfate radical, UV, Water treatment

Background

Cyanobacteria are the most diverse and widespread phototrophic prokaryotes inhabiting earth for several billions of years [1, 2]. Cyanobacteria can be found almost everywhere in terrestrial and aquatic environments, even in Antarctic lakes and hot springs [3]. Due to their dependence on nutrients and temperature, the increasing eutrophication of waterbodies and climate change promote more frequently and extensively occurring cyanobacterial blooms [2, 4–6]. Although not all blooms are poisonous, at least 40 cyanobacterial species are known to produce diverse secondary metabolites that are toxic to biota including plants [7], animals and humans. Consequently, cyanobacteria and their toxins pose a major risk to surface waters intended for drinking and recreational purposes, and adequate measures must be employed to prevent or eliminate cyanobacterial blooms and toxins.

The first approach should prevent the occurrence of cyanobacterial blooms in surface water by measures such as nutrient reduction, biomanipulation or the application of algaecides [4, 8]. Importantly, especially in the case of toxic cyanobacteria, the removal of intact cyanobacterial cells is essential to avoid the release of intracellular toxins, e.g., microcystins (MCs), anatoxin-a (ANTX) and saxitoxin (STX) [6, 9].

The second approach is the removal of cyanobacterial cells and metabolites in drinking water treatment facilities. Although most conventional drinking water

*Correspondence: marcel.schneider@recetox.muni.cz; marcel.schneider90@outlook.com
RECETOX, Faculty of Science, Masaryk University, Kamenice 753/5, 62500 Brno, Czech Republic

Springer Open

© The Author(s) 2020. This article is licensed under a Creative Commons Attribution 4.0 International License, which permits use, sharing, adaptation, distribution and reproduction in any medium or format, as long as you give appropriate credit to the original author(s) and the source, provide a link to the Creative Commons licence, and indicate if changes were made. The images or other third party material in this article are included in the article's Creative Commons licence, unless indicated otherwise in a credit line to the material. If material is not included in the article's Creative Commons licence and your intended use is not permitted by statutory regulation or exceeds the permitted use, you will need to obtain permission directly from the copyright holder. To view a copy of this licence, visit http://creativecommons.org/licenses/by/4.0/.

treatment methods effectively remove cyanobacterial cells and intracellular metabolites, extracellular and dissolved cyanotoxins may bypass conventional methods such as rapid sand filtration and coagulation [2]. Hence, adequate and more advanced treatment measures must be implemented to ensure sufficient removal of cyanotoxins. While traditional treatment approaches such as physical retention, biodegradation or chemical oxidation can be effective, they all come with various practical, economic or environmental disadvantages.

Toxin removal by physical retention can be achieved by filter membranes with very low molecular weight cut-off pore sizes, i.e., nanofiltration and reverse osmosis, or adsorbents like activated carbon and bioadsorbents [10]. However, when dissolved cyanotoxins are only physically removed, appropriate measures for the disposal or further treatment of the toxin-enriched retentate are required. In addition, filter beds and membranes may need to be backwashed regularly to prevent clogging, fouling and cyanobacterial growth on the filter medium [10, 11].

Although several cyanotoxins are biodegradable [12], their periodical occurrence may limit the microorganisms' ability to degrade cyanotoxins, resulting in an initial lag-phase of up to a few days without pre-conditioning [10, 12]. Moreover, most enzymatic degradation mechanisms are still poorly understood which makes it difficult to predict the effectiveness of a biological treatment barrier [10, 12] and potential drawbacks such as the biotransformation of the less-toxic gonyautoxin (GTX) into the more toxic STX [12].

Although commonly used oxidants such as chlorine and permanganate effectively degrade some cyanotoxins, others are not susceptible or require oxidant concentrations and reaction times that are substantially higher than those usually applied in drinking water treatment [2, 9, 13]. As a major disadvantage, chlorination can produce halogenated disinfection byproducts formed from the reaction of chlorine with organic matter or in the presence of bromide [14]. Furthermore, residual chlorine may impair the drinking water quality due its possibly perceptible taste and odor. Permanganate on the other hand does neither promote the formation of toxic disinfection byproducts, nor produce taste or odor, but it tints the water pink at >0.05 mg L^{-1}, which limits its application and residual concentration in drinking water [10].

As another form of oxidation, advanced oxidation processes (AOPs) have received a lot of attention for their application in drinking and wastewater treatment for the degradation of even recalcitrant organic compounds and disinfection of pathogens. In AOPs, reactive species, mainly ·OH, and other mechanisms are formed in situ [10]. This review gives a detailed insight into AOPs which were investigated for cyanotoxin removal from drinking water to evaluate their feasibility and applicability. Therefore, we briefly outline current regulations for cyanotoxins in drinking water and basic principles of different AOPs. Following, we discuss the most relevant findings from the scientific literature on the degradation effectiveness, advantages and disadvantages of individual methods and the role of relevant water quality parameters. From there, information gaps are identified and recommendations for future research for the effective removal of cyanotoxins from drinking water are formulated.

Cyanobacterial toxins

Cyanotoxins can cause a vast range of clinical signs, including acute hepatotoxicosis, peracute neurotoxicosis, gastrointestinal disturbances as well as respiratory and allergic reactions [6]. Many different cyanobacterial metabolites can be considered cyanotoxins [15]. Here, we will only focus on cyanotoxins for which information on their removal from drinking water was found.

Microcystins

Microcystins are the most commonly studied cyanotoxins produced by different cyanobacteria such as *Microcystis, Nostoc*, *Planktothrix* and many other species [16]. This group of water soluble cyclic heptapetides consists of more than 100 congeners which exhibit similar toxicological properties due to their akin chemical structure, which mainly differs in two amino acids *X* and *Z* (Fig. 1) [6]. Hence, MCs are named according to these two variable amino acids, e.g., MC-LR with *X* and *Z* being leucine (L) and arginine (R), respectively. The hydrophobic Adda amino acid is often associated as the key structural element for MCs' biological activity [14]. Unless cyanobacterial cells lyse due to extrinsic stress or senescence, MCs are usually intracellular. In the presence of bacteria and photosynthetic pigments, dissolved MCs rapidly degrade in natural waters [6]. Depending on the degree of sunlight, content of natural organic matter (NOM) and presence of bacteria, MCs can have a half-life of 4 to 14 days in surface water [17].

Nodularin

Nodularin (NOD) and its seven analogs are cyclic pentapeptides produced by *Nodularia* and *Nostoc* strains. NOD's structure (Fig. 1) is similar to MC, leading to similar chemical and toxicological characteristics [6, 16]. Similar to MC, the hepatotoxic NOD is also intracellular until the bloom starts to decay [6].

Cylindrospermopsin

Cylindrospermopsin (CYN) was first isolated from *Cylindrospermopsis raciborskii* and later from other species

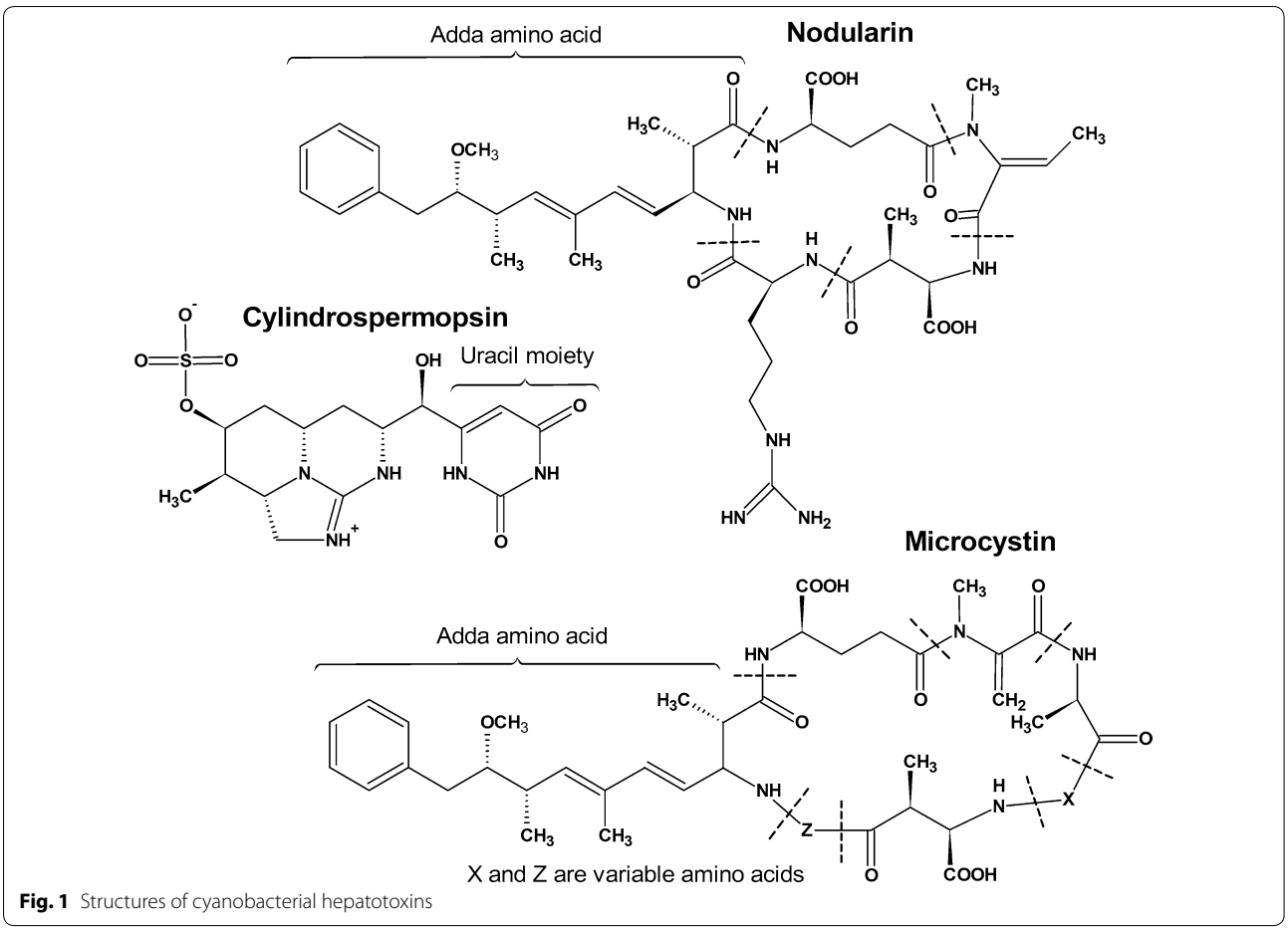

Fig. 1 Structures of cyanobacterial hepatotoxins

including *Aphanizomenon* and *Oscillatoria*. So far, five analogs of this highly water soluble and planar-shaped alkaloid have been described (Fig. 1) [18, 19]. CYN is extracellular and is relatively stable to a wide range of heat, light and pH conditions. The alkaloid can persist in water for more than a month [6, 18]. However, when exposed to sunlight in the presence of cell pigments, CYN has a half-life of about 0.6 to 0.9 days [17].

Anatoxins

Anatoxin-a (Fig. 2) and its derivatives are produced by *Aphanizomenon*, *Dolichospermum* (formerly *Anabaena*), *Oscillatoria* and *Planktothrix*. The extremely potent alkaloid neurotoxin acts as a cholinergic nicotinic agonist causing nerve depolarization and neuromuscular blockage. ANTX is usually intracellular, but rapidly degrades once it is released from cells and is exposed to natural sunlight (half-life of approximately 100 min) and oxidants. However, in the absence of sunlight, ANTX can reach a half-life of several days to months. Main degradation products of ANTX and homoanatoxin-a are the notably less-toxic dihydro- and epoxy analogs [9, 17, 20].

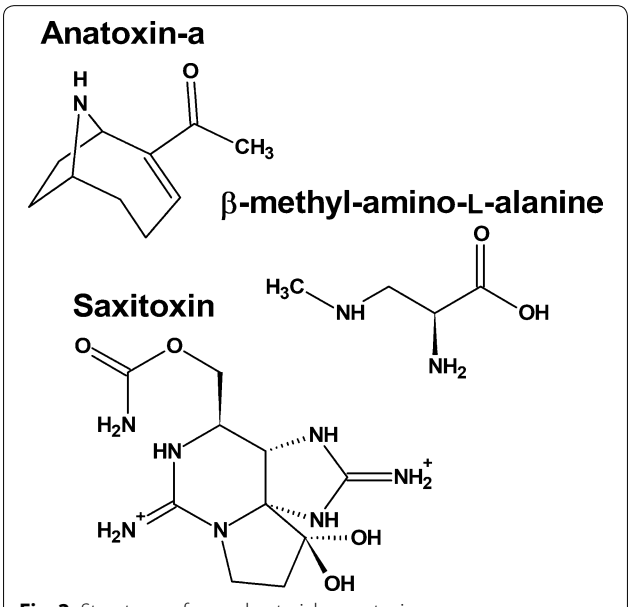

Fig. 2 Structures of cyanobacterial neurotoxins

Saxitoxins

STX, also known as paralytic shellfish toxin, is produced by organisms from different taxonomic kingdoms—eukaryotic dinoflagellates and prokaryotic cyanobacteria. Cyanobacterial producers include *Aphanizomenon*, *Cylindrospermopsis, Dolichospermum* and *Lyngbya* [21]. STX can be substituted at various positions (Fig. 2), resulting in currently 57 known analogs, which can be grouped into non-sulphated STXs, singly sulfated GTXs and doubly sulfated C-toxins. The toxicity of the STXs analogs inversely increases with the number of substituted sulfates [12, 21]. Because of its two cationic guanidine groups, the alkaloid is water soluble [9]. Unless cyanobacterial cells lyse, STX is usually intracellular [9].

β-*N*-methylamino-L-alanine

β-*N*-methylamino-L-alanine (BMAA) is a non-proteinogenic amino acid (Fig. 2) reported to be present in terrestrial and marine, free-living and plant symbiotic cyanobacteria including *Aphanizomenon*, *Cylindrospermopsis*, *Microcystis* and *Nodularia* [22]. The possible association of BMAA with several neurotoxic outcomes is discussed in the literature, e.g., by Ploux et al. [22] and references cited therein.

Exposure to cyanobacterial toxins and current regulations for drinking water

The presence of harmful cyanobacterial blooms and their toxins can evidently be traced back to the nineteenth century, where poisoning through ingestion of surface water led to sickness and death of livestock, pets and wildlife [23]. Ever since, cyanobacterial blooms and toxins have reportedly caused several, partly fatal incidents around the globe. In 1979, more than 100 people were poisoned and had to be hospitalized in Queensland, Australia due to the consumption of contaminated drinking water. Further investigations identified the water supply and later determined *Cylindrospermopsis raciborskii* as the source for the poisoning, which is now known as the Palm Island mystery disease [24]. Almost 20 years later, 76 hemodialysis patients died in Brazil due to the utilization of water contaminated with MCs and CYN for hemolysis treatment [25]. Besides posing a risk to human health, cyanotoxins can also have economic consequences [26]. Due to a massive *Planktothrix rubescens* bloom in the Serbian Vrutci reservoir with cell counts of about 10,000 cells L^{-1} in the treated drinking water in December 2013, Serbian authorities prohibited the use of tap water in the city of Užice, Serbia (approximately 70,000 inhabitants). As a result of the incapability to remove cyanobacterial cells and toxins, an alternative, cyanobacteria-free water source—Sušičko vrelo reservoir—had to be used for several years until reconstruction of the Vrutci reservoir treatment facility was completed [27]. In a similar, but more far-reaching incident, the Ohio EPA put a temporary ban on tap water for the city of Toledo, Ohio, USA in August 2014. About 500,000 people were advised not to drink or otherwise use tap water after MC concentrations in the drinking water exceeded the regulatory threshold of 1 μg L^{-1}. After a few days, when MC concentrations decreased to below the limit, the ban was lifted [28, 29].

To protect humans from exposure to cyanotoxins through consumption of contaminated drinking water, adequate treatment measures must be employed. However, even if effective removal techniques are in place, a comprehensive drinking water guideline, containing a thorough monitoring and actions' program, is indispensable. A set of threshold values can thus help to take actions in case they are exceeded. So far, the WHO suggested a provisional guideline value (GV) for MC-LR of 1 μg L^{-1} based on a total daily intake (TDI) of 0.04 μg kg^{-1} day^{-1} derived from acute toxicity data [30]. However, GVs for others cyanotoxins have not been proposed yet due to the lack of toxicological and epidemiological data. The upcoming update on the WHO Guidelines for Drinking-water Quality, to be published in 2020–2021, is expected to include recommendations for ANTX, CYN and STX as well as a revision of the GV for MC. Updates can be found on the homepage [31]. The currently proposed GV for MC-LR was accepted or adapted by many countries across the globe [32]. The lack of toxicological and epidemiological data on effects of exposure to other cyanotoxins also raises the question on effects from cyanotoxin mixtures and chronic exposure. The US EPA was the first to propose a chronic TDI (0.003 μg kg^{-1} day^{-1}) for MC-LR and lowered their acute TDI (0.006 μg kg^{-1} day^{-1}) based on updated data [16].

AOPs for cyanotoxin removal from drinking water

Although many different reactive chemical species can be produced, short-lived ·OH is often considered to be the most important species generated in AOPs in water, most likely due to its comparably high reactivity as indicated by its redox potential (Table 1). This non-selectively and randomly attacking oxidant primarily reacts with organic compounds in two distinctive mechanisms: (i) via an electrophilic attack at electron-rich moieties such as C=C double bonds, aromatic systems and neutral amines, and (ii) via hydrogen abstraction from C–H groups [33]. At neutral pH, ·OH can also react in an often kinetically disfavored one-electron transfer mechanism [34].

The following sections address the existing knowledge on the removal of different cyanotoxins by AOPs in detail. We were able to identify studies that investigated the use of hydrogen peroxide, ozone, photolysis

Table 1 Redox potentials of commonly used oxidants indicating their reactivity

Oxidant	pH range	Redox potential in V/SHE
Sulfate radical (SO_4^{-})	Acidic to neutral	2.5–3.1[a]
Hydroxyl radical (·OH)	Acidic	2.7[a]
	Neutral to alkaline	1.8[a]
Ferrate ($[FeO_4]^{2-}$)	Acidic	2.2[b]
	Alkaline	0.7[b]
Ozone (O_3)	Acidic	2.1[a]
	Alkaline	1.2[a]
Peroxydisulfate ($S_2O_8^{2-}$)	Acidic	2.0[a]
Hydrogen peroxide (H_2O_2)	Acidic	1.8[a]
	Alkaline	0.9[a]
Peroxymonosulfate (HSO_5^- or SO_5^{2-}, $pK_a = 9.4$[c])	Acidic	1.8[a]
Hydroperoxy radical (HO_2·)	–	1.7[d]
Permanganate (MnO_4^-)	Acidic	1.7[a]
	Alkaline	0.6[a]
Hypochlorous acid (HOCl)	–	1.5[c]
Chlorine (Cl_2)	–	1.4[d]
Chlorine dioxide (ClO_2)	–	1.3[d]
Peroxymonosulfate radical (SO_5^-·)	Neutral	1.1[c]
Sulfite radical (SO_3^-·)	Neutral	0.6[c]

SHE standard hydrogen electrode

[a] [35]

[b] [10]

[c] [36]

[d] [13]

(including the combination with oxidants and catalysts), Fenton oxidation, non-thermal plasmas, sulfate radicals, electrochemical oxidation, sonolysis and radiolysis.

Hydrogen peroxide

Although H_2O_2 has a higher redox potential than, e.g., chlorine under acidic conditions (Table 1) and is often used as a precursor for ·OH as well as to improve the effectiveness of AOPs, it is relatively ineffective for the degradation of cyanotoxins if employed solely. Removal of MC-LR, CYN, ANTX and BMAA by H_2O_2 was reported to be < 10% [37–41]. Even at 30 °C for 3.5 h, only about 3% MC-LR was removed by H_2O_2 [36].

Ozonation and O_3-based AOPs

Ozonation is widely employed in drinking water treatment for disinfection of microorganisms and oxidation of various organic pollutants [42]. Even though ozonation itself technically is not an AOP as O_3 is usually produced in the gaseous phase, we discuss it in this review, because O_3 can be used as an AOP precursor and it decomposes to ·OH in situ under alkaline conditions (Eqs. 1 and 2) [2, 43]. Ozone itself has a relatively high redox potential at acidic pH (Table 1) and reacts with organic compounds in a similar but more selective manner compared to ·OH. It attacks electron-rich groups such as unsaturated C=C, aromatic systems and neutral amines [9]. Numerous studies showed the high effectiveness of O_3 for the degradation of MCs, NOD, CYN, ANTX and BMAA [14, 19, 37, 44–46]). On the other hand, ozonation is not recommended for STXs degradation, as the toxicity to mice of an STX extract treated with O_3 and O_3/H_2O_2 was reduced by < 10% only [47].

$$O_3 + OH^- \rightarrow HO_2^- + O_2 \quad (1)$$

$$O_3 + HO_2^- \rightarrow \cdot OH + O_2^- \cdot + O_2 \quad (2)$$

$$Fe^{2+} + O_3 \rightarrow FeO^{2+} + O_2 \quad (3)$$

$$FeO^{2+} + H_2O \rightarrow Fe^{3+} + \cdot OH + OH^- \quad (4)$$

$$O_3 + O_2^- \cdot \rightarrow O_3^- \cdot + O_2 \quad (5)$$

$$CO_3^{2-} + \cdot OH \rightarrow CO_3^- \cdot + OH^- \quad (6)$$

$$HCO_3^- + \cdot OH \rightarrow CO_3^- \cdot + H_2O \quad (7)$$

$$O_3 + \cdot OH \rightarrow HO_2 \cdot + O_2 \quad (8)$$

Ozone can be used as an AOP precursor in combination with other oxidants, UV light (see the section on "Photolysis in combination with oxidants"), catalysts and adsorbents, which increase ·OH formation. One of the most commonly used and comparatively cheap O_3-based AOPs is the peroxone process, in which O_3 reacts with deprotonated H_2O_2 to produce ·OH (Eq. 2). This process has been shown to further increase the degradation of MCs and ANTX compared to O_3 alone [44, 45]. Similarly, degradation of both toxins also increased when Fe^{2+} was combined with O_3 (Eqs. 3 and 4) [44, 45]. However, the combination of O_3 with the Fenton's reagent (see the section on "Fenton oxidation") only improved MC-LR degradation at low O_3 concentrations due to the oxidation of Fe^{2+} at higher levels [48]. Instead of Fe^{2+}, the commonly used photocatalyst TiO_2 can also be used. CYN degradation improved by almost 30% when O_3 was combined with TiO_2 due to increased O_3 decomposition to ·OH and CYN adsorption to the catalyst [49].

With regard to water quality parameters, pH plays an important role because it can affect both the toxin speciation and the oxidant, influencing thus the treatment

effectiveness. Although O_3 reactivity with the conjugated diene in MCs' Adda amino acid was shown to be pH-independent, reactions with the amine and uracil moiety in ANTX and CYN, respectively, depend on the pH in consistence with the toxins' pK_a value [14, 19]. In contrast, Al Momani et al. [45] observed a substantially reduced MC-LR degradation when increasing the pH from 2 to 11. This indicates that not only toxin speciation, but also reactivity and availability of dissolved ozone are pH-dependent. Under alkaline conditions, O_3 redox potential decreases by almost 50% (Table 1) and ozone decomposition to ·OH increases (Eqs. 1, 2 and 5). In addition, if ·OH quenching by NOM and alkalinity (as carbonate/bicarbonate, Eqs. 6 and 7) is reduced due to low availability, ozone consumption is further promoted by ·OH (Eq. 8) [43]. BMAA degradation with O_3 was also observed to be pH-dependent but direct O_3 attack was less important, while secondary oxidants such as HO_2^- formed from O_3 under alkaline conditions (Eq. 1) played a substantial role [37]. Moreover, the selectivity of O_3 toward specific electron-rich moieties was shown to be pH-dependent, as the C=C double bonds in CYN and ATNX are primarily attacked at pH < 7–8, whereas oxidation of the amine groups dominates at higher pH [14, 19, 46]. Overall, reaction rate for the ozonation at pH 8 was in the order of MC-LR > CYN > ANTX [19].

Besides ·OH quenching, NOM may also quench O_3. In the presence of 2 mg L^{-1} humic acid, MC-LR and -RR degradation by O_3 reduced by approximately 25% [45]. In fact, NOM concentration was shown to be more influential on the degradation than its composition and alkalinity [19, 49]. In addition to water quality parameters discussed above such as pH, alkalinity and NOM, the actual concentration of cyanotoxins and other pollutants dictates the O_3 demand of water. However, the effects of water quality on the pollutant removal are neglectable once a residual O_3 concentration is present in the treated water. Hence, an ozone residual of > 0.3 mg L^{-1} for ≥ 5 min, which is typically applied in water treatment plants, is recommended for cyanotoxin removal [2].

Photolysis

Photolysis occurs in the environment by exposure to sunlight and is commonly employed for disinfection in water treatment utilizing UV light. Upon absorption of light, energy is released from a molecule through physical and chemical processes which include the breakdown of a compound [50]. Although ANTX readily degrades under sunlight in absence of photosensitizers ($t_{1/2}$ = 1–2 h at alkaline pH) [51], other cyanotoxins such as MCs and CYN are less susceptible to direct photodegradation by sunlight [52]. Efficacy of photolytic treatment strongly depends on the wavelength, i.e., energy of the used light. For instance, ANTX has an absorption maximum in the range of 230–240 nm, which determines the toxin's resistance to UV-A irradiation (315–400 nm), while it degrades by 70% under UV-C irradiation at 254 nm [39]. Similarly, NOD degradation also improved when UV light of a shorter wavelength, i.e., higher energy, was used [53]. With vacuum-UV at 172 nm, water is directly photolyzed to form ·OH (Eq. 9), which further increased ANTX degradation and substantially reduced the UV dose required for complete removal. However, direct water photolysis is strongly limited to a light penetration depth in water of < 100 µm, which makes ·OH formation by vacuum-UV less attractive to drinking water treatment compared to other AOPs [54].

$$H_2O + hv\ (172\ nm) \rightarrow H_2O^* \rightarrow H\cdot + \cdot OH \quad (9)$$

Besides wavelength, light intensity is a crucial parameter as well. MC-LR degradation increased by about 30–40% when light intensity was tripled [55]. Moreover, at 254 nm and a dose of 564 mJ cm^{-2}, approximately 66% MC-LR degradation was achieved, while at 312 nm, a much higher dose of 11,304 mJ cm^{-2} was required to yield similar results [55, 56]. In addition to irradiation, degradation also depends on the toxin structure as shown in a study on UV-photolytic treatment of four MCs, where degradation increased from MC-LR < -RR < -YR < -LA owing to the different amino acid structures (A = alanine, L = leucine, R = arginine, Y = tyrosine) [41].

UV-based treatments are so far the only methods for which MC-LR detoxification due isomerization of the 4(E),6(E)-Adda chain (Fig. 1) to 4(Z)- or 6(Z)-Adda was observed. Furthermore, degradation mechanisms include decarboxylation, which has only been reported for UV-based methods and sulfate radical-based AOPs (SR-AOPs; see the section on "Sulfate radical-based AOPs") [56, 57].

Cyanotoxins usually co-occur with NOM which can act as photosensitizer and improve the degradation. For instance, MC-RR photodegradation by sunlight substantially increased in presence of the cyanobacterial pigment phycocyanin [58]. However, photosensitizer concentration is essential as it was shown for MC-LR degradation. At lower concentrations, pigment availability was the limiting factor, while at higher concentrations, light attenuation was significant [59]. In a similar manner, ANTX photodegradation was more effective in the presence of NOM but the degradation decreased with increasing NOM concentration. Experiments with quenchers showed that besides excited NOM, $^1O_2$ and ·OH also contributed to the toxin degradation and that $^1O_2$ was more important than ·OH [60]. In contrast, photosensitized CYN degradation was observed to be mainly driven by ·OH (about

65–70%), with $^1O_2$ and excited NOM only playing minor roles [61]. This disagreement may not only be related to the different toxins, but also to experimental conditions and using fulvic acid and solar light vs humic acid and UV-C light, respectively. Although phycocyanin did not improve CYN photodegradation, other cyanobacterial compounds were observed to accelerate NOD and CYN degradation [53, 62, 63]. In fact, the presence of different pigment types was shown to affect MC-LR photodegradation effectivity in the following order: without pigment < chlorophyll a < β-carotene < water-extractable pigments < solvent-extractable pigments [58]. Furthermore, higher light intensities led to pigment bleaching and degradation which adversely affected MC-LR degradation [59].

Turbidity is one of the most important water quality parameters for photodegradation. Light absorption by non-target water constituents not acting as photosensitizer attenuates light and reduces penetration depth. Therefore, photodegradation is usually efficient in relatively clear water, after most turbidity has been removed [10]. Other water quality parameters may also affect the degradation as shown for ANTX degradation by UV-C radiation, where toxin removal was more effective at acidic pH with an optimum at pH = 6.4, most likely due to ANTX speciation under acidic conditions ($pK_a = 9.4$) and possible inter- and intramolecular hydrogen bonding under alkaline pH. Also, higher temperatures led to increased ANTX degradation, but the changes became insignificant at $T > 24$ °C. Last, as for most AOPs, alkalinity was observed to decrease ANTX degradation due to quenching of reactive species [60].

To achieve high degradation yields, UV doses substantially higher than those commonly used for disinfection in water treatment (10–40 mJ cm^{-2} [9]) are required. Consequently, to reduce energy demand and operating costs for large-scale water treatment, the combination of UV with oxidants or photocatalysts—as discussed in the following paragraphs—is inevitable.

Photolysis in combination with oxidants

The combination of UV radiation with H_2O_2 or O_3 improves pollutant degradation due to the photolytic production of ·OH (Eqs. 10 and 11) [56]. Moreover, ·OH and $SO_4^{-}\cdot$ are produced from peroxymonosulfate (PMS) or peroxydisulfate (also persulfate, PS) upon UV activation (see the section on "Sulfate radical-based AOPs"). In a UV/chlorine system, ·OH, Cl·, OCl· and other reactive species are formed following Eqs. (12) to (16) [64].

$$O_3 + H_2O + hv \rightarrow O_2 + H_2O_2 \quad (10)$$

$$H_2O_2 + hv \rightarrow 2 \cdot OH \quad (11)$$

$$HOCl + hv \rightarrow \cdot OH + Cl\cdot \quad (12)$$

$$OCl^- + hv \rightarrow O^- \cdot + Cl\cdot \quad (13)$$

$$Cl \cdot + Cl^- \rightarrow Cl_2^-\cdot \quad (14)$$

$$HOCl/OCl^- + \cdot OH \rightarrow H_2O/OH^- + OCl\cdot \quad (15)$$

$$HOCl/OCl^- + Cl\cdot \rightarrow HCl/Cl^- + OCl\cdot \quad (16)$$

$$\cdot OH + H_2O_2 \rightarrow \cdot HO_2 + H_2O \quad (17)$$

UV in combination with oxidants has been studied for the removal of MCs, CYN, ANTX and BMAA. For all for toxins, UV-based treatment was substantially more effective when H_2O_2 was added [37, 39, 40, 54, 55, 60]. Increasing H_2O_2 concentration improved cyanotoxin degradation only up to a certain oxidant concentration. Once the optimal H_2O_2 level was exceeded, ·OH quenching by H_2O_2 (Eq. 17) outbalanced radical formation [54, 55, 60]. Different studies reported that MCs were degraded at higher rates compared to CYN, ANTX and BMAA because of their higher reactivity with ·OH. This is caused by MCs' size and higher number of functional moieties that are partly more susceptible to radical attack [37, 41, 65]. The importance of the structure for the reactivity with ·OH is further affirmed when looking at different MCs. The major part of their structures is similar with the main difference being two amino acids (see Fig. 1). However, these minor differences suffice to yield different degradation rate constants: MC-YR (1.63×10^{10} M^{-1} s^{-1}) > MC-RR (1.45×10^{10} M^{-1} s^{-1}) > MC-LR (1.13×10^{10} M^{-1} s^{-1}) > MC-LA (1.10×10^{10} M^{-1} s^{-1}) [41].

When O_3 was added to UV instead of H_2O_2, MC-LR degradation also became more effective compared to UV- and O_3-only treatment. O_3 decomposition to ·OH is accelerated under UV irradiation and as a consequence, both O_3 and ·OH oxidize pollutants [56, 66]. Although O_3, i.e., its production, may be more expensive compared to H_2O_2 and TiO_2 (for UV/TiO_2 see the section on "Photocatalysis"), to achieve similar results, shorter reaction times and lower oxidant doses were required compared to UV/H_2O_2 treatment [56]. Due to the UV irradiation, decarboxylation and isomerization of MC-LR were observed, which did not occur in O_3-only treatment. Furthermore, compared to UV- and O_3-only treatment, UV/O_3 had a higher potential to degrade MC-LR and its degradation intermediates simultaneously under the same conditions [56].

As another, cheaper alternative to H_2O_2, the addition of chlorine has been studied in UV-based AOPs [67].

UV/chlorine was shown to be more effective compared to UV/H_2O_2, UV- and chlorine-only MC-LR treatment. Besides producing a variety of reactive oxygen and chlorine species (Eqs. 12 to 16), Cl· is more selective than ·OH and preferably reacts with electron-rich moieties [64]. Similar to UV/H_2O_2, increasing the chlorine dose led to a more effective MC-LR degradation due to an increase in reactive chlorine species production and higher contribution to toxin degradation [64, 67]. However, the use of chlorine may lead to the formation of halogenated degradation products such as chloroform and dichloroacetic acid produced from MC-LR following a series of oxidation steps [67]. Even though yields of these chlorinated byproducts increased with prolonged treatment time, residual cytotoxicity after UV/chlorine treatment was lower compared to untreated MC-LR [67].

Besides oxidant type and dose, the UV radiation itself is an important factor, as the peroxide bond in H_2O_2 is cleaved only upon irradiation with light of $\lambda < 300$ nm [39]. Hence, MC-LR and ANTX degradation by UV-A/H_2O_2 ($\lambda_{UV\text{-}A} \approx 400–315$ nm) has been reported to be substantially less effective compared to UV-B/H_2O_2 and UV-C/H_2O_2 ($\lambda_{UV\text{-}B} \approx 315–280$ nm, $\lambda_{UV\text{-}C} \approx 280–100$ nm), respectively [39, 55, 68].

Similar to other AOPs, water quality parameters can influence UV/oxidant degradation efficacy. In the UV/oxidant setup NOM rather acts as oxidant and radical quencher than as photosensitizer, thus decreasing removal efficacy, which is in contrast with NOM action during photolysis without the addition of oxidants. NOM may compete with the oxidant for UV photons which consequently reduce reactive species formation [60, 65, 69]. The UV/O_3 system was also affected by NOM but to lesser extent than O_3-only treatment of MC-LR [56]. In case of UV/chlorine degradation of MC-LR, NOM did not only decrease the degradation, but also resulted in a higher yield of chlorinated byproducts. This yield was observed to be dependent on NOM as well as chlorine dosage [67]. In the presence of bromide, MC-LR degradation increased due to the formation of HOBr which is more reactive than HOCl toward phenolic and amine moieties. Furthermore, UV activation of HOBr formed reactive bromine species which may have contributed to MC-LR degradation [64]. Alkalinity decreased UV/H_2O_2 and UV/chlorine degradation efficacy similar to NOM due to H_2O_2 and radical quenching [64, 69].

UV/oxidant removal efficacy is also affected by water pH. For ANTX removal by UV/H_2O_2, the highest efficacy was achieved at pH 6.7, while at lower pH the ·OH yield decreased due to reactions with H^+ and at alkaline pH ANTX is deprotonated and exists as neutral amine ($pK_a = 9.4$). In this form, inter- and intramolecular hydrogen bonds can form which affect ANTX reactivity with ·OH [39]. In contrast, for BMAA removal, alkaline pH appeared to increase the degradation rate constant due to BMAA speciation at higher pH [37]. In UV/O_3 systems, the pH does not only determine toxin speciation, but also O_3 stability, which decreases at alkaline pH and may affect toxin degradation. However, this effect seemed to be less influential for MC-LR degradation by UV/O_3 compared to O_3-only treatment [56]. In UV/chlorine-based treatment, the oxidant itself is also strongly affected by the pH, when HOCl dissociates to OCl^- at alkaline pH ($pK_a = 7.5$). OCl^- has a lower molar absorption and thus a lower radical yield. Furthermore, OCl^- reacts at a higher rate with ·OH and Cl· compared to HOCl. The optimum pH for MC-LR degradation by UV/chlorine was determined to be pH 7.4 [67]. In contrast, in another study MC-LR degradation by UV/chlorine was shown to be most effective at pH 6 and decreased at pH 7 [64]. Most of the experimental conditions seemed to be very similar, i.e., oxidant type and concentration, UV wavelength, MC-LR concentration and pH-buffer composition but notable differences were the UV intensity and pH-buffer concentration, which could have affected the outcomes. Both studies also examined the contribution of different reactive species to MC-LR degradation and reported different findings. In the first study, at neutral pH, MC-LR degradation by UV/chlorine was dominated by ·OH (42.5%), while Cl_2 (25.4%), ClO· (13.3%), Cl· (11.1%) and UV (8.5%) contributions were lower [67]. In the second study, at neutral pH, MC-LR degradation was driven by HOCl/OCl^- (47.3%), while reactive chlorine species (21.3%), UV (21.1%) and ·OH (10.3%) were only partially responsible for MC-LR degradation. Also in the second study, the UV intensity was about twice as high compared to the first study, which may explain the difference in the higher UV contribution [64].

Photocatalysis

Instead of oxidants, photoactive semiconductors can be used to improve UV-based cyanotoxin degradation. Upon exposure to light with energy exceeding the band gap between occupied valence band and unoccupied conductance band, an electron migrates from the valence to the conductance band. The formed valence band hole yields an oxidative site, while the now occupied conductance band provides a reducing site. As a result, three reaction mechanisms are possible: (i) direct oxidation at the valence band, (ii) ·OH formation from H_2O or OH^- at the valence band, and (iii) O_2^{-}· and subsequent H_2O_2 formation from O_2 at the conductance band [70].

Photocatalysis was shown to be effective for the removal of MCs, NOD and CYN [71–74]. Besides toxin degradation, adsorption onto the catalyst is often reported as a fourth removal mechanism. In a study with

different MCs, degradation was faster, when adsorption to the catalyst was the highest [75], while in another study, no correlation of MC and NOD degradation with dark adsorption was observed [74]. In the first study, TiO_2 powder was used as received [75], while in the second study, the catalyst was coated onto glass spheres [74], which may have caused these contradicting findings. Effectivity of dark adsorption depends on toxin composition and hydrophobicity in particular. Adsorption to TiO_2 increased with increasing pollutant hydrophobicity and was thus pH-dependent, caused by compound speciation and change of hydrophobicity at certain pH. Hence, for MCs, adsorption increases at acidic pH [75, 76].

Because of its high oxidizing power, chemical stability and low cost, TiO_2 is a commonly used photocatalyst [70]. Toxin degradation is accelerated with increasing TiO_2 concentration, but levelled off once a certain catalyst concentration was reached [72–74]. However, TiO_2 is only photoactive at UV light, which limits its applicability. Therefore, TiO_2 has been doped with mostly non-metal elements to reduce the band gap and consequently decrease the energy required for its activation [77]. Although N-doped TiO_2 was less effective than pure TiO_2 under UV and solar light, MC-LR could only be removed under visible light with N-TiO_2 [73]. Further, N-F-co-doped TiO_2 achieved higher removal compared to N- or F-TiO_2 under visible light [77]. For the removal of 6-hydromethyl uracil, a CYN model compound, under UV light, degradation efficacy for different co-doped TiO_2 was in order: N-F-TiO_2 > P-F-TiO_2 > S-TiO_2, while N-F-TiO_2 was the only catalyst which removed the uracil derivative under visible light [78]. MC-LR could be removed by Vis/S-TiO_2 due to the different toxin structure, allowing MC-LR adsorption to the photocatalyst and consequently allowing for degradation [79]. Similarly, C-doped TiO_2 showed lower removal rates under UV light compared to pure TiO_2, but in contrast, achieved MC-LR and CYN degradation under visible light. Differences in the reaction products and reactive species involved revealed distinct reaction mechanisms under UV and visible light [71]. Under UV light, ·OH was the primary reactive species, while under visible light, O_2^{-}· became more important [71, 78, 80]. Besides doped TiO_2, other photocatalysts, e.g., WO_3 and Fe_2O_3 showed high response to solar light and were used for MC-LR degradation [81, 82]. Similar to TiO_2, doping of WO_3 improved MC-LR degradation and dopants can be ordered according to the removal rate: WO_3 < CuO–WO_3 < Pd–WO_3 ≪ Pt–WO_3 [81]. When BiOBr was used as photocatalyst, MC-LR and CYN degradation was achieved by direct reaction with the catalyst instead of radicals, which followed a different reaction mechanism, involving decarboxylation [83, 84].

A major limitation of photocatalysis is the need to remove the catalyst in a subsequent treatment step, which becomes even more difficult if nano-scale powder is used. Hence, employing heterogeneous or immobilized photocatalysts improves or avoids removal and makes photocatalysis more attractive for large-scale water treatment. Besides substrates like glass or PVC, cellulose acetate and PET monoliths were found to be the best supporting materials for TiO_2 photocatalytic treatment of MC-LR and CYN [85]. When coated onto granular-activated carbon, TiO_2 photocatalysis of MC-LR improved compared to pure TiO_2 powder due to increased adsorption to TiO_2 or to activated carbon sites in vicinity to the catalyst [86]. In case of Fe-based photocatalysts, immobilization to a substrate is evitable because they can be separated magnetically [82].

Similar to photolysis, photocatalysis efficacy depends on the light characteristics, i.e., wavelength and intensity in particular. Although doped TiO_2 is also activated under visible light, degradation rates are reduced by two to three orders of magnitude compared to UV or solar light [71, 73]. With higher light intensities, more electron–hole pairs are formed regardless of the employed photocatalyst, which results in higher toxin removal [72, 81].

When UV/TiO_2 was combined with H_2O_2, higher MC-LR degradation was achieved compared to UV/TiO_2 or UV/H_2O_2 alone [87]. Although dark adsorption to the catalyst decreased in the presence of the oxidant, H_2O_2 decomposition to ·OH increased when TiO_2 was present. However, H_2O_2 concentration was shown to be a crucial factor, as the MC-LR degradation rate was highest at 0.005% H_2O_2 in solution and decreased at higher concentrations [87]. Besides adding oxidants, photocatalysis can also be enhanced when used in photoelectrocatalysis. Similar to elemental doping of a photocatalyst, photoelectrocatalysis improves the photocatalytic activity by removing electrons from the catalyst to reduce the recombination of electron–hole pairs to instead utilize the holes in the conductance band for oxidant production and pollutant reduction [88]. Under given experimental conditions, MC-LR degradation was substantially more effective by photoelectrocatalysis using Ag/AgCl/TiO_2 nanotube electrodes compared to photocatalysis and electrochemical degradation alone [89]. Because this approach is based on an electrolytic cell, parameters such as electrolyte composition affect the degradation and need to be optimized (see the section on "Electrochemical oxidation").

Also for photocatalytic toxin removal, water quality parameters such as pH and NOM have major an impact. For instance, regardless of type and doping of the photocatalyst, higher MC and CYN removal was achieved

under acidic conditions [72, 76, 82]. However, when different scavengers were used during MC-LR degradation by Vis/NF–TiO_2, the solution pH did not only affect dark adsorption, but also played a crucial role in the formation and reactivity of reactive oxygen species [80]. Although NOM can act as photosensitizer in photolysis, it may adsorb to the catalyst surface and quench reactive species produced by photocatalysis which reduces toxin removal. Similarly, high alkalinity quenches and thus limits ·OH availability [76]. Another crucial water quality parameter is dissolved O_2 which functions as precursor for O_2^{-}· and H_2O_2 formation at the conductance band. Under O_2-free atmosphere, cyanotoxin degradation substantially decreased or was completely inhibited [72, 78]. In the presence of Fe^{3+} and Cu^{2+}, toxin degradation increased due to ·OH production in a Fenton-like reaction [78, 81] (see the section on "Fenton oxidation"). At lower concentrations, Cl^- can function as a precursor for Cl· which was shown to increase MC-LR degradation. However, when exceeding an optimal Cl^- concentration, ·OH quenching and Cl_2 formation became more efficient and suppressed toxin degradation [81].

Fenton oxidation

In a Fenton reaction ·OH is produced via the reaction shown in Eq. (18). The Fenton's reagent thereby refers to Fe^{2+}/H_2O_2, but other transition metals, e.g., chromium, copper, manganese as well as other oxidants, e.g., HClO, $S_2O_8^{2-}$ or HSO_5^- can also produce ·OH or SO_4^{-}· in Fenton-like reactions (see the section on "Sulfate radical-based AOPs" for SO_4^{-}· production") [36, 90]. Fenton oxidation of several cyanotoxins was studied, and the removal effectiveness was found to be in order of MC-RR > CYN > MC-LR ≫ ANTX > STX [36, 38, 44, 45, 91, 92].

$$Fe^{2+} + H_2O_2 \rightarrow Fe^{3+} + \cdot OH + OH^- \quad (18)$$

$$Fe^{3+} + H_2O_2 \rightarrow Fe^{2+} + HO_2 \cdot + H^+ \quad (19)$$

$$Fe^{3+} + HO_2\cdot \rightarrow Fe^{2+} + O_2 + H^+ \quad (20)$$

$$Fe^{2+} + \cdot OH \rightarrow Fe^{3+} + OH^- \quad (21)$$

The Fe^{2+} to H_2O_2 ratio is among the most crucial parameter that must be optimized to prevent parasitic reactions which inhibit ·OH formation. In case of H_2O_2 excess, Fe^{3+} is reduced to Fe^{2+} at a slower rate as the Fenton reaction, consuming H_2O_2 to yield HO_2· (Eqs. 19 and 20). The formation of the less reactive HO_2· is competing with the formation of more reactive ·OH (Table 1). An excess in H_2O_2 also leads to the formation of HO_2· by ·OH depletion (Eq. 17). In addition, ·OH can be quenched by an excess of Fe^{2+} (Eq. 21) [90]. Several studies reported different optimal Fe^{2+} to H_2O_2 ratios, even for the same toxins, which emphasizes that experimental conditions like toxin concentration and solution pH must be considered [38, 44, 45, 93].

Fenton oxidation is often reported to be most effective at pH ≈ 3 [90]. At alkaline pH, Fe^{2+} forms hydroxides which tend to precipitate, thus reducing Fe^{2+} availability to produce ·OH [38]. Furthermore, H_2O_2 stability decreases at alkaline pH which further limits ·OH formation [94]. On the other hand, under too strong acidic conditions, H^+ inhibits Fe^{3+} reduction which also decreases Fe^{2+} availability [93]. For practical applications, treatment closer to neutral pH may be beneficial as it would reduce resources and costs required for pH adjustments before and after Fenton treatment while keeping a sufficient effectiveness, e.g., 77% MC-LR removal at pH 3 and 68% removal at pH 5, [38]. To extend the pH range, heterogeneous or immobilized catalysts can be used which additionally improves its removability from water. For instance, across a pH range of 5–8 in a photo-Fenton process, heterogeneous FeY was shown to yield a higher catalytic activity than Fe^{2+} [95]. Although alkaline pH is often reported to decrease Fenton effectiveness due to lower ·OH yields, the formation of alternative oxidants at neutral and alkaline pH was proposed in a study with Reactive Black 5 and As^{3+} [96]. Oxidation increased again under alkaline pH which was associated with high-valent iron species, i.e., Fe^{4+}, in form of hydroxo-complexes [96].

In Fenton-like reactions, transition metals and oxidants other than Fe^{2+} and H_2O_2 produce ·OH. For instance, Fe^{3+} can be used instead of Fe^{2+}. However, MC-LR degradation was shown to be significantly slower, because Fe^{3+} first is reduced to Fe^{2+} by H_2O_2 (Eqs. 19 and 20) before it eventually produces ·OH [97]. Besides MC-LR, CYN and ANTX were also shown to be degraded by a Fenton-like system, namely Fe^{3+}, which was bond to a macrocyclic ligand system, in combination with H_2O_2 [91]. In another study, Cu^{2+} in combination with ascorbic acid was used to degrade MC-LR. Ascorbic acid reduced Cu^{2+} to Cu^+ which then activated O_2 to form H_2O_2 via O_2^{-}·. Cu^+/H_2O_2 produced ·OH at a rate of approximately 100 M^{-1} s^{-1} which is in a similar range as the Fe^{2+}/H_2O_2 system (76 M^{-1} s^{-1}) [98].

Fenton oxidation can be improved when combined with UV/Vis light which leads to photoreduction of Fe^{3+} to Fe^{2+} as well as photolytic ·OH generation from H_2O_2 [68]. Photo-Fenton was shown to be more effective compared to dark Fenton MC-LR degradation due to combined effects of photolytic and Fenton mechanisms [99]. Due to the continuous photoreduction of Fe^{3+} and photocatalytic ·OH generation from Fe^{3+} in form of $Fe(OH)^{2+}$, UV-C/Fe^{3+}/H_2O_2 was more effective than UV-C/Fe^{2+}/

H_2O_2 for the degradation of MC-LR [68]. Furthermore, the spectrum of the irradiation light was also shown to affect MC-LR degradation, as UV-C and solar light were more effective than UV-A [68, 100]. Other hybrid Fenton techniques use ultrasound or electrolysis (for electro-Fenton see the section on "Electrochemical oxidation") to improve pollutant removal. In sono-Fenton, ·OH formation is further accelerated by combining sonochemical (see the section on "Sonolysis") and Fenton mechanisms [101].

As for most AOPs, NOM quenches produced ·OH and may thus reduce the effectiveness of Fenton oxidation [38]. Although CYN degradation by Fenton oxidation decreased in the presence of NOM, the effect appeared to be less extensive compared to, e.g., ozonation and UV/TiO_2 [92]. Photo-Fenton may be more affected by NOM due to light attenuation [68]. However, the effect of NOM on the degradation strongly depends on its type and composition. The removal rate of MC-LR by solar photo-Fenton in presence of different NOM types was in the order of fulvic acid > NOM-free > humic acid > a mixture of fulvic and humic acids plus bicarbonate as alkalinity. Humic acid usually has a larger molecular weight and contains more aromatic moieties than fulvic acid which, in turn, may act as a chelating agent, stabilizing Fe^{2+} [102]. Similarly, when zero-valent iron nanoparticles were used in a heterogeneous Fenton-like reaction, humic acid seemed to form H_2O_2-cleaving iron complexes which resulted in higher MC-LR degradation [103].

Non-thermal plasma

Low or atmospheric pressure plasmas in which most of the energy is transmitted to free electrons (temperatures of $\geq 10^4$ K), while the remaining heavy species only receive minor amounts of energy (temperatures of $\leq 10^3$ K), are called non-thermal plasmas (NTPs). A broad spectrum of reactive species is generated by NTPs, including hot electrons, photons, and heavy species such as radicals, excited atoms, molecules and ions, reactive oxygen and nitrogen species. In addition, some discharges may generate shock waves [104, 105]. NTPs are generated by electric discharges in the gaseous or liquid phase, or at their interface and due to the overall low plasma temperature can be employed in many different fields including water treatment [104, 106]. In fact, because of higher efficiencies compared to other means of O_3 production, O_3 generators are often based on electric discharges in air or oxygen [106].

For an electric discharge in gas, the gas type and composition dictate which reactive species are produced. For a discharge in air or oxygen, one of the most important processes is O_3 formation. However, in the presence of N_2, i.e., in discharges in air, NO_x are also produced, which lead to acidification and nitrification of the solution if the gas is bubbled through water afterward [107]. O_3 produced in gas can directly react with pollutants or dissolve into the liquid when the gas is bubbled through the solution after the discharge, where it can also decompose to ·OH [108]. If oxygen-free gases such as Ar are used, no reactive oxygen species are produced in the gas phase, but when the gas passes through water, ·OH can be formed upon reaction with ionized or excited species in the gas [109]. In electric discharges in water, low-energy electrons excite water molecules, whereas high-energy electrons dissociate water. Both reactions lead to the formation of ·OH (Eqs. 22 and 23), which is one of the main reactive species produced by a discharge in water. H_2O_2 is formed as a recombination product of ·OH [107]. With a discharge in liquid, reactive species can directly react with pollutants in the plasma channels or close to the plasma–liquid boundary without the need to diffuse from the gaseous into the liquid phase [110]. For an electric discharge at the gas–liquid interface, plasma channels usually form on top of the liquid surface as the liquid acts as counter electrode. Here, reactive species are formed in the gaseous and liquid phases and can easily diffuse into the other phases [111, 112].

$$H_2O^* + H_2O \rightarrow H\cdot + \cdot OH + H_2O \quad (22)$$

$$e^- + H_2O \rightarrow H^- + \cdot OH \quad (23)$$

So far, NTPs were studied for the removal of MCs, ANTX and BMAA [108, 109, 111–115]. Besides the type of reactive species produced in an electric discharge, other parameters also affect the treatment efficacy. Studies on MC-LR removal in a gas–liquid surface discharge showed that a higher operating voltage increased the degradation due to a higher energy input [111, 115], and similar results were shown for the degradation of ANTX in a dielectric barrier discharge in O_2 and subsequently bubbling the gas through the sample solution [108]. Here, an increased operating voltage led to higher O_3 concentrations, which in turn also resulted in higher ·OH levels in water due to decomposition of dissolved O_3 [108]. However, for discharges in air, maximal O_3 concentration may not be achieved with the highest voltage, because of increasing O_2 consumption in NO_x reactions and O_3 depletion in reactions with N and NO at higher voltages [116]. Besides operating voltage, pH was also shown to affect the MC-LR degradation effectiveness in an Ar–water surface discharge, in which an acidic pH was beneficial for the removal [109]. Since MC-LR was expected to be unaffected in the studied pH range, the ·OH concentration was assumed to be reduced under alkaline pH due to reaction with OH^- [109]. The concentrations

of the formed reactive species can also be increased by higher gas flow rates [115].

The electrode distance also impacts the plasma chemistry, when decreasing distance between high-voltage electrode and the water surface, the energy increases and intensifies the reactions induced by the plasma. For a shorter electrode distance, the transfer time into the solution is reduced especially for short-lived reactive species [111, 112, 115], where long transfer times can reduce the degradation effectiveness. This is why catalysts have been studied as additives in NTPs to transform long-lived species like O_3 and H_2O_2 into the more reactive ·OH. For example, Mn-doped carbon xerogels not only increase the ·OH concentration, but also adsorb, e.g., MC-LR, thus immobilizing the toxin to enhance reactions with oxidants [112, 114]. Because electric discharges also generate UV light, photocatalysts like TiO_2 have also been studied as additives to increase the formation of ·OH (see the section on "Photocatalysis") [114]. Due to the formation of H_2O_2 in water, another alternative is the addition of Fe^{2+} to yield the Fenton's reagent (see the section on "Fenton oxidation") [115]. Plasma generation, intensive heat and direct electro-physical and -chemical processes at the electrode can lead to corrosion, resulting in the release of metal ions from the electrodes. Correspondingly, electrodes made from catalytic active materials may release, e.g., Fe^{2+} from stainless steel, which, in combination with H_2O_2 produced by the discharge, increases thus ·OH formation [107].

Besides pollutant degradation during the actual treatment, plasma treated water has been shown to yield residual—post-treatment—oxidative and microbicidal effects. Up to a few days after exposure to an electric discharge, plasma-treated water still effectively degraded for example BMAA [113]. Although this phenomenon is still not fully elucidated, long-lived reactive species such as O_3, H_2O_2 and peroxynitrous acid (HNO_3) may be responsible for this residual effect [104].

When simulating a real water matrix by adding, for example, K_2HPO_4, $NaNO_3$ or humic acid, degradation of MC-LR was reduced due to competition for ·OH [109]. For ANTX degradation by a dielectric barrier discharge in O_2, KNO_3, KH_2PO_4 and glucose were shown to affect the degradation similarly [108].

Sulfate radical-based AOPs

In SR-AOPs, $SO_4^{-}\cdot$ is the major reactive species generated from PMS or PS. It is more selective than ·OH and has a higher redox potential at neutral pH (Table 1), which may make it more suitable for water treatment across a broader pH range [35, 36, 117]. Furthermore, PS and PMS are more stable than H_2O_2, increasing precursor transportability across longer distances within water [117]. Moreover, the peroxide bond in PS has a lower bond dissociation energy which requires less energy for radical production compared to H_2O_2 [118]. $SO_4^{-}\cdot$ can be generated by cleaving the peroxide bond in PMS and PS using energy-based activations through heat, UV irradiation, ultrasound and plasma (Eqs. 24 and 25) [35, 117, 119]. Activation of PMS and PS in redox reactions can be achieved using transition metals in a Fenton-like mechanism (see the section on "Fenton oxidation"), O-functionalized activated carbon, electrochemical processes, radiolysis (e^- formation in water, Eq. 46) and ozone (Eqs. 26–33) [35, 117, 120, 121]. Unexpectedly, phosphate-buffered saline (PBS), a commonly used pH-buffer, was also shown to activate PMS, and the PBS/PMS system effectively degraded model water pollutants Acid Orange 7, rhodamine b and 2,4,6-trichlorophenol [122].

$$HSO_5^- + \text{energy input} \rightarrow SO_4^-\cdot + \cdot OH \tag{24}$$

$$S_2O_8^{2-} + \text{energy input} \rightarrow 2SO_4^-\cdot \tag{25}$$

$$HSO_5^- + e^- \rightarrow SO_4^-\cdot + \cdot OH \ (\text{or } SO_4^{2-} + \cdot OH) \tag{26}$$

$$S_2O_8^{2-} + e^- \rightarrow SO_4^-\cdot + SO_4^{2-} \tag{27}$$

$$SO_4^{2-} \rightarrow SO_4^-\cdot + e^- \tag{28}$$

$$\text{AC surface} - OOH + S_2O_8^{2-} \rightarrow SO_4^-\cdot + \text{AC surface} - OO\cdot + HSO_4^- \tag{29}$$

$$\text{AC surface} - OH + S_2O_8^{2-} \rightarrow SO_4^-\cdot + \text{AC surface} - O\cdot + HSO_4^- \tag{30}$$

$$SO_5^{2-} + O_3 \rightarrow SO_5^-\cdot + O_3^-\cdot \left(\text{or } SO_4^{2-} + 2O_2\right) \tag{31}$$

$$SO_5^-\cdot + O_3 \rightarrow SO_4^-\cdot + 2O_2 \tag{32}$$

$$SO_5^-\cdot \rightarrow 2SO_4^-\cdot + O_2 \left(\text{or } S_2O_8^{2-} + O_2\right) \tag{33}$$

$$O_3^-\cdot + H_2O \rightarrow \cdot OH + OH^- + O_2 \tag{34}$$

$$SO_4^-\cdot + H_2O \rightarrow SO_4^{2-} + \cdot OH + H^+ \tag{35}$$

$$SO_4^-\cdot + OH^- \rightarrow SO_4^{2-} + \cdot OH \tag{36}$$

$$SO_4^-\cdot + \cdot OH \rightarrow HSO_5^- \tag{37}$$

$$HSO_4^- + OH\cdot \rightarrow SO_4^- \cdot + H_2O \quad (38)$$

$$H_2SO_4 + \cdot OH \rightarrow SO_4^- \cdot + H_3O^+ \quad (39)$$

SR-AOPs are a worthy alternative to ·OH-based AOPs due to the simultaneous generation of ·OH as secondary radical when PMS is used as precursor (Eqs. 24 and 26), in the presence of water (Eq. 35), under alkaline conditions (Eq. 36) or when PMS is activated using O_3 (Eqs. 31 to 34). Consequently, ·OH is the primary reactive species at alkaline pH, whereas $SO_4^{-}\cdot$ is the dominant radical at acidic pH. At neutral pH, both radicals equally contribute to pollutant oxidation [117, 121]. The reaction of both radicals forms PMS (Eq. 37), which in turn can again be activated to generate $SO_4^{-}\cdot$ and ·OH [117]. In addition, the reaction of ·OH with HSO_4^- or H_2SO_4 can also produce $SO_4^{-}\cdot$ (Eqs. 38 and 39) [120].

$SO_4^{-}\cdot$ generally reacts with organic pollutants in three distinctive routes: (i) via hydrogen abstraction from C–H bonds, (ii) via addition to unsaturated bonds and (iii) via electron transfer reactions from carboxylates, amines and aromatic compounds [35]. The third mechanism promotes decarboxylation, which, besides for SR-AOPs, has only been reported for UV-based degradation of cyanotoxins [56, 83, 84, 121, 123]. PMS and PS also function as oxidants, but $SO_4^{-}\cdot$ is usually more effective and faster given its substantially higher redox potential (Table 1). PS is usually preferred over PMS due to its higher stability, water solubility, photosensitivity and is more frequently used in standard methods and commercial instruments [35].

SR-AOPs have been studied for the removal of MCs, CYN and ANTX, mainly focusing on UV and catalyst activation [36, 40, 41, 124]. Even without activation, high removal ($\geq$ 90%) of MC-LR and CYN was achieved after > 500 min of treatment for PS and > 100 min of treatment for PMS, while ANTX was almost unaffected by PMS without activation. However, when UV radiation was added, degradation of these three toxins became more effective [40, 41, 124]. MC-LR and CYN degradation efficacy was in order of UV/PS > UV/PMS > UV/H_2O_2 [40, 41]. Due to its structure, MC-LR was faster degraded than CYN because it provides more moieties prone to radical attack [40, 41]. Studies with different MC variants showed that under UV only, degradation increased following MC-LR < -RR < -YR < -LA, while the differences were only small in the presence of PMS, PS or H_2O_2 [41]. Similar to MC-LR and CYN, degradation efficacies for MC-LA, -RR and -YR followed UV/PS > UV/PMS > UV/H_2O_2 > UV-only [41]. Similar to other photolytic AOPs, the wavelength influenced the degradation efficacy in UV-activated SR-AOPs. For example, ANTX removal increased when the wavelength was decreased from 290 to 260 nm [124]. A follow-up experiment with radical quenchers revealed that under the experimental conditions used, ANTX degradation was dominated by $SO_4^{-}\cdot$ [124].

In contrast to UV activation, MC-LR degradation efficacy was in a different order: Co^{2+}/PMS (pH = 5.8) > Fe^{2+}/H_2O_2 (pH = 3) ≫ Ag^+/PS (pH = 5.8) because PMS accepts e^- more easily than H_2O_2 and PS [36]. Moreover, activation of PS requires substantially higher transition metal concentrations [36, 125].

MC-LR degradation was further improved by addition of TiO_2 to the UV/PMS or UV/PS system due to photolytic and photocatalytic (see the section on "Photocatalysis") production of $SO_4^{-}\cdot$ and ·OH [126], and addition of transition metals can promote (photo-) Fenton-like mechanisms. For instance, Cu^{2+} and Fe^{2+} improved CYN degradation by UV/PMS, even in the presence of NOM [40]. Similar results were observed for ANTX, and again, UV/PMS/Cu^{2+} yielded better results compared to UV/PMS/Fe^{2+} [124]. Besides type and properties of the activation mechanism, an increase in the oxidant concentration seems to generally increase the degradation rate due to the formation of more reactive species [36, 40, 124].

As for other AOPs, water quality parameters may considerably influence cyanotoxin degradation by SR-AOPs. Reaction rate constants of $SO_4^{-}\cdot$ with NOM were shown to be two orders of magnitude lower compared to rate constants of ·OH with NOM but quenching effects can still occur and particularly depend on NOM composition and concentration [40, 125]. For ANTX degradation by UV/PMS, $\leq$ 2 mg L^{-1} of NOM was shown to improve toxin removal due to photosensitization. But at higher NOM concentrations, radical scavenging outbalanced this photosensitizing effect, and inhibited ANTX degradation [124]. Interestingly, humic acid and quinones, which are active functional humic acid moieties, were shown to activate PS and effectively degraded for example PCB28 [127]. Hence, NOM may not only act as photosensitizer, but also certain moieties may eventually react with PS to produce $SO_4^{-}\cdot$.

Besides NOM, alkalinity can also act as radical scavenger, especially since carbonate and bicarbonate concentrations (mg L^{-1}) highly exceed toxin concentrations (μg L^{-1}) in surface water [40, 124]. The pH of the treated water is another important factor which determines the speciation of toxins, catalysts as well as oxidants. In UV/SR-AOPs at acidic conditions around pH 3, MC-LR degradation rate constants substantial increased compared to unbuffered solutions with pH 4.8 and pH 6.4 for PMS and PS, respectively [36]. ANTX removal by UV/PMS, on the other hand, was most effective at pH 6.4 and decreased under more acidic (pH 3.0) and alkaline conditions (pH 8.0) [124]. However, when the Co^{2+}/

PMS system was acidified, MC-LR removal decreased from 100% after 5 min at pH = 5.8 to 27% after 60 min at pH = 3 and became substantially less effective compared to the Fenton reagent at pH = 3 [36]. This decrease in MC-LR degradation is rather caused by inhibition of PMS decomposition than reduced reactivity of $SO_4^{-}\cdot$ at acidic pH.

Electrochemical oxidation

In an electrolytic process, pollutant oxidation can occur directly, via electron transfer to the anode surface and indirectly, via electrochemically formed reactive species including ·OH, H_2O_2, O_3 (Eqs. 40–42) and others depending on electrolyte composition, which is why it is also referred to as electrochemical AOP (EAOP). Based on the setup of the treatment cell, EAOPs can be grouped into four different classes. The simplest is direct and indirect anodic oxidation (AO) of a pollutant. At neutral or acidic pH and in the presence of air or O_2, H_2O_2 can additionally be generated by cathodic reduction (Eq. 43, AO-H_2O_2). To further increase the treatment, Fe^{2+} can be added to yield ·OH (electro-Fenton, EF). In EF, continuous cathodic electrogeneration of H_2O_2 and cathodic Fe^{3+} regeneration to Fe^{2+} (Eq. 44) perpetually produce the Fenton's reagent if an undivided cell is used (see the section on "Fenton oxidation"). If EF is exposed to light (photoelectro-Fenton, PEF), the Fenton reaction itself can be improved by photolytic H_2O_2 cleavage to ·OH (see the sections on "Photolysis" and "Fenton oxidation"). In EAOPs, non-active anodes with high O_2-overpotential (potential for O_2 development) such as boron-doped diamond anodes (BDD) are usually employed. The higher the O_2-overpotential, the weaker is the physisorption of ·OH to the anode surface, which, in turn, leads to higher ·OH availability in the solution [90].

$$M + H_2O \rightarrow M(\cdot OH) + H^+ + e^- \quad (40)$$

$$2M(\cdot OH) \rightarrow 2MO + H_2O_2 \quad (41)$$

$$3H_2O \rightarrow O_3 + 6H^+ + 6e^- \quad (42)$$

$$O_{2(g)} + 2H^+ + 2e^- \rightarrow H_2O_2 \quad (43)$$

$$Fe^{3+} + e^- \rightarrow Fe^{2+} \quad (44)$$

Here, M(·OH) means ·OH is physisorbed to the anode surface M. Electrochemical oxidation of MC, NOD and CYN has been investigated with different electrodes and treatment parameters [120, 128–131]. One of the most influential factors in terms of degradation effectiveness and operating costs are the electrodes used in EAOPs. BDDs are often used due to their high O_2-overpotential, and regardless of the used electrolytes, achieved higher MC-LR degradation compared to mixed metal oxide electrodes such as IrO_2–Ta_2O_5/Ti [130]. Even when coated onto Ti as carrier material, MC-LR removal was in order of Ti/BDD > Ti/IrO_2 > Ti/Pt > Ti/SnO_2 under otherwise same conditions [129]. However, BDD electrodes are costly and cheaper alternatives such as electrodes synthesized from nanosized TiO_2 coated onto a graphite carrier were efficient for MC-LR degradation [128].

Besides electrode material, the applied current affects the degradation efficacy with higher current densities resulting in higher toxin removal [120, 129]. The efficacy of an EAOP also depends on the electrolyte composition and its electric conductivity. For instance, MC-LR degradation in filtered lake and tap water improved after increasing the conductivity by adding Na_2CO_3 [128, 132]. The electrolyte composition also dictates which reactive species are produced and thus, EAOPs can be tailored toward specific requirements and pollutants. Although the order of cyanotoxin removal for electrolyte salts is usually $Cl^- > SO_4^{2-} > NO_3^- > CO_3^{2-}$ [129, 133, 134], SO_4^{2-} is often suggested as best choice because of lower production of toxic disinfection byproducts from halogen-based electrolytes and avoidance of eutrophication from N- and P-based electrolytes [129, 134]. The risk of halogenated byproducts can be reduced at low salt concentrations and higher current densities but this would, in turn, increase electric energy demand [133].

Influence of water parameters on degradation of cyanotoxins by EAOPs has only scarcely been investigated but studies showed NOM scavenging of produced reactive species [130]. For the effect of pH on MC-LR degradation by EAOPs, contradicting observations were reported. While Zhang et al. [135] found no significant effect on MC-LR degradation rate constants across a range of pH from 5 to 9, Zhou et al. [130] observed higher MC-LR degradation at lower pH. Both studies used different electrolytes ($NaNO_3$ and Na_2SO_4, respectively), which may explain the different results. In a photoelectrocatalytic treatment of MC-LR using Ag/AgCl/TiO_2 nanotubes electrodes, the degradation appeared to be pH-dependent due to more effective adsorption to TiO_2 under acidic pH and a lower potential level of the valence band of the photoelectrode at alkaline pH which decreased MC-LR oxidation [89].

Sonolysis

In sonolysis, ultrasound is used to form liquid-free cavities, i.e., bubbles, in a liquid medium due to rapid changes in pressure created by an oscillating ultrasonic wave. When these bubbles collapse, high energy is released

in form of average bubble temperatures of 4200 K and pressures of 500 atm [10]. Volatile and nonpolar pollutants can be degraded in the cavitation by direct pyrolysis, thermolysis, hydrolysis or hydroxylation with ·OH formed from the gas-phase thermolysis of water (Eq. 45) [10]. Besides acoustically, i.e., due to ultrasound, cavities can also be formed hydrodynamically, where cavities are generated when a liquid is forced to flow under reduced pressure which leads to a local drop of the static pressure to below the critical value. This can be achieved, e.g., by a local increase of the flow rate, flow line curvature or channel constrictions [136].

$$H_2O \xrightarrow{)))} H\cdot + \cdot OH \quad (45)$$

Non-volatiles and compounds with an amphiphilic or less polar character are degraded in the interfacial boundary layer between the bubble and bulk where temperatures of up to 2000 K and high ·OH concentrations are present. Non-volatile and polar compounds are degraded in the bulk aqueous phase by ·OH migrating away from the cavitation or H_2O_2 formed in the system [10]. The degradation effectiveness thus depends on the pollutant's physico-chemical properties and preferred chemical environment, i.e., polar/nonpolar or volatile/non-volatile [137]. Besides pyrolysis, thermolysis and chemical reactions, shockwaves and high shear forces are released, which can be utilized to, e.g., destruct and lyse cyanobacterial cells [10]. Depending on the pollutant and desired processes, the ultrasonic wave frequency can be adjusted to favor formation and reactions of ·OH (200–600 Hz) or higher temperatures and pressures (< 200 Hz) [10].

So far, studies focused solely on the sonolytic treatment of MCs [137–140], and the highest degradation was observed in the approximate frequency range of 150–410 kHz. Both lower and higher frequencies resulted in less effective degradation due to lower ·OH concentrations [139, 140]. An increase in the applied power yielded higher MC degradation but the degradation rate was substantially faster only in the first few minutes of the treatment and later became undistinguishable when comparing 30, 60 and 90 W [140]. In addition to the power (in W) or intensity (in W cm^{-2}), the distribution of the ultrasound within the treated area affects the treatment efficiency [10]. A study with different radical scavengers showed that about 39% of the degradation was achieved by ·OH in the bulk solution and about 35% degradation was achieved by ·OH at the bubble interface [138]. Due to its non-volatile and polar character, MC-LR is not expected to reside inside the cavity but the nonpolar Adda side chain most likely resides in the bubble interfacial region [138]. MC-LR degradation can be improved under acidic conditions that increase the hydrophobicity of the Adda moiety [137]. Some MC degradation can also be attributed to hydrolysis and pyrolysis in the interfacial region, while shear forces are unlikely to cause mechanical destruction of the toxin [138]. Also, H_2O_2 is produced in sonolytic processes and can act as a quencher reducing the MC-LR degradation, it can simply be overcome by adding Fe^{2+}, which eliminates H_2O_2 and further increases ·OH formation (for the section on "Fenton oxidation") [137]. Interestingly, NOM, e.g., from cyanobacterial cells, appeared to only have a small effect on the treatment effectivity [138].

Radiolysis

Radiolysis uses ionizing radiation with energies of approximately 100 eV, which is substantially higher than energies usually required for ionization of organic compounds (< 15 eV) and cleavage of chemical bonds (1–5 eV) [141]. Commonly used radiation sources are radionuclides and electrostatic accelerators emitting γ-radiation and electron beams, respectively [141, 142]. Radiolysis requires specialized instrumentation and expertise which are rare in water treatment facilities. However, because it produces a range of reactive chemical species in water and no precursors or other additives are needed, it can be useful for in-depth studies of oxidation mechanisms. The radiolytic decomposition of water is shown in the following equation (radiation yields G (in μmol J^{-1}) are given in parentheses) [142, 143]:

$$H_2O \xrightarrow{rad} e^-_{aq}(0.27) + \cdot OH(0.28) + H\cdot(0.06) + H_2(0.05) + H_2O_2(0.07) + H_3O^+(0.27) + HO_2\cdot(0.003) \quad (46)$$

So far, only studies with MCs, CYN and ANTX used radiolysis [19, 143–145]. The rate constants for ·OH attacking specific functional moieties of MC-LR were determined in the following order: benzene ring in Adda moiety (10^{10} M^{-1} s^{-1}) ≥ diene in Adda moiety (10^{10} to 10^9 M^{-1} s^{-1}) > aliphatic hydrogens (10^8 M^{-1} s^{-1}) [143]. Although hydrogen abstraction is the slowest reaction pathway, it is still assumed to be significant due the large number of > 50 potential reaction sites [143]. The overall calculated rate constant for the reaction of ·OH with MC-LR (using literature values for appropriate surrogates, mainly amino acids) 2.1×10^{10} M^{-1} s^{-1} [143] is very close to the experimentally derived rate constant 2.3×10^{10} M^{-1} s^{-1}, for which the ·OH attack at the Adda group accounted for almost 70% in the model [143]. For CYN, the overall rate constant of 5.1×10^9 M^{-1} s^{-1} was measured with the uracil side chain being the main susceptible moiety for ·OH attacks (84%), whereas the attack at the guanidine group is less important [61]. In another

study, the rate constants for the reaction of ·OH with MC-LR and CYN using radiolysis were determined to be within the same order of magnitude, 1.1×10^{10} M^{-1} s^{-1} and 5.5×10^{9} M^{-1} s^{-1}, respectively [19]. The negligibly different factors are most likely caused by differences in the experimental conditions and methodologies used in the different studies. The order of rate constants was found to be MC-LR > CYN > ANTX, which corresponds to the toxins' molecular size and number of H-atoms that can be abstracted by ·OH [19].

The efficiency of radiolytic treatment of MCs is dose-dependent and can be improved by adding Na_2CO_3 or H_2O_2 which leads to the formation of HO_2· and ·OH, respectively [144]. In contrast, nitrite and nitrate were shown to decrease the removal due to scavenging of ·OH [144]. Furthermore, since ·OH is a non-selective oxidant, radiolytic treatment can obviously be impacted by water quality parameters such as NOM [19, 145].

Comparison of AOPs

Degradation efficiency of AOPs

When comparing different AOPs, especially considering their application in large-scale water treatment, degradation efficiency is among the most crucial parameters. It relates the required energy, oxidant or catalyst dose to the efficacy of the treatment. For energy efficiency of AOPs, electrical energy per order (E_{EO}) is often chosen as a figure of merit. E_{EO} is defined as electrical energy in kWh required to remove a pollutant by 1 order of magnitude, i.e., 90%, in 1 m^3 of water [146]. In case of oxidants or catalysts, the "stored electric energy" of a compound can be calculated based on prices for electric energy (price per kWh) and the respective compound (price per kg) [147].

Based on a comprehensive review on AOPs for water treatment and data on their energy efficiency reported in peer-reviewed literature, Miklos et al. [146] grouped established and emerging AOPs according to their E_{EO} values (Fig. 3). According to this review, most reported E_{EO} values did not include auxiliary oxidants or catalysts in the calculations. The first group comprises AOPs with median E_{EO} values of < 1 kWh m^{-3} which represents a realistic range for full-scale application. The second group includes AOPs with median E_{EO} values of 1–100 kWh m^{-3} which is energy extensive but in case of specific problems, these AOPs may provide an attractive solution, also for eventual large-scale applications. The last group contains AOPs with median E_{EO} values of > 100 kWh m^{-3} which are currently not considered to be energy efficient [146]. Nevertheless, future developments may lead to optimization and reduction of energy demands and related costs.

E_{EO} values for cyanotoxin removal by AOPs have only rarely been reported. For UV/H_2O_2 treatment of MC-LR and CYN, E_{EO} values were 4.5×10^{-3}–6.1×10^{-3} and 1.6×10^{-3} kWh m^{-3}, respectively [40, 148]. For UV/PMS and UV/PS treatment, E_{EO} values were estimated to range from 10^{-4} to 10^{-5} kWh m^{-3}, respectively, for CYN, and 0.7 and 0.2 kWh m^{-3}, respectively, for MC-LR [40, 126]. For electrochemical oxidation of MC-LR, the E_{EO} ranged from 48 to 67 kWh m^{-3} depending on electrode material [129]. These E_{EO} values seem to agree with the results by Miklos et al. [146]. However, for UV/TiO_2 treatment, low E_{EO} values, approximately 0.08 to 0.14 kWh m^{-3}, were reported for MC-LR and 0.03 to 0.015 kWh m^{-3} for MC-LR, -LA and -RR in two independent studies [126, 149] which are at least 2–3 orders of magnitude lower compared to the results by Miklos et al. [146]. Although energy-efficient UV-LEDs were used in the second study [149], the light source itself seems not to have a substantial effect since demanding UV xenon lamps were used in the study of Antoniou et al. [126].

Interestingly, process capacity, i.e., laboratory-, pilot- and full-scale application, was inversely correlated with E_{EO} values which decreased with increasing

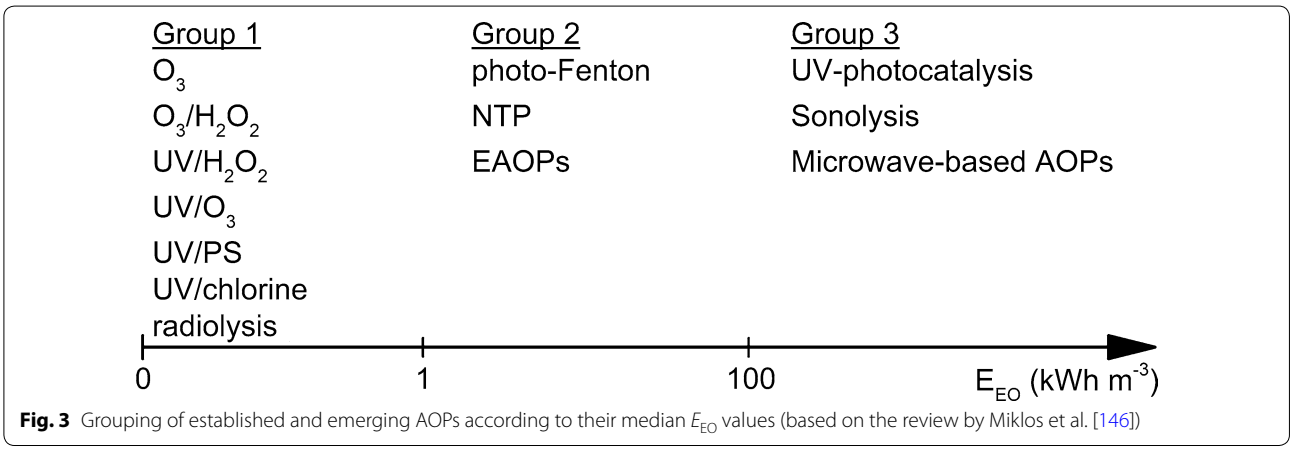

Fig. 3 Grouping of established and emerging AOPs according to their median E_{EO} values (based on the review by Miklos et al. [146])

process capacity. This indicates that up-scaling apparently improves energy efficiency and the demands derived from laboratory-scale experiments may not be correctly translated to full-scale processes. Furthermore, water quality (pure, drinking, ground- and wastewater) did not affect E_{EO} values significantly, even when relevant parameters such as NOM, UV transmittance and turbidity were considered [146].

Potential of disinfection byproduct formation

An important aspect is the formation of toxic disinfection byproducts (DBPs) during AOP treatment, where halogenated organic and inorganic compounds such as trihalomethans, haloacetic acids, haloacetronitrils, chlorates, bromates and others are of special concern [146]. Because of their toxicity, the WHO recommended guideline values for several DBPs like chloroform (300 µg L^{-1}), bromoform (100 µg L^{-1}), perchlorate (70 µg L^{-1}) and bromate (10 µg L^{-1}) [150–152]. DBP formation depends on the employed AOP as well as the water matrix, i.e., presence of nitrogen, organic matter and halogens [146].

Formation of bromate is relevant for O_3 and O_3-based AOPs, where up to 50% of bromide (at concentrations > 100 µg L^{-1}) can be converted to bromate [146], and ·OH may promote bromate formation by about 30–70% [153]. Attenuation is possible by decreasing pH, O_3 or bromide concentration and in the presence of H_2O_2 [153, 154]. Chlorate formation by O_3 and O_3-based AOPs may only be relevant if the treatment contains a pre-chlorination step [146].

In most ·OH-dominated AOPs, bromate formation can usually be neglected in the abundance of organic matter or H_2O_2 due to radical quenching [146, 154]. Chlorate and perchlorate are only produced under specific conditions when reactive chlorine species are abundant, which may further react with organic matter to form halogenated DBPs. Generally, DBP formation by ·OH is considered to be noncritical with the exception for some approaches like high-density ·OH generation at electrode surfaces in EAOPs [146].

For SR-AOPs, bromate formation is effectively inhibited by small concentrations of organic matter [146, 154] but reactions of SO_4^{-}· with chloride may produce Cl· and subsequently chlorate at pH < 5 [154].

UV irradiation does not produce inorganic DBPs but can form nitrite due to photolysis of nitrate which may subsequently lead to the formation of nitrated aromatic compounds. In UV/chlorine processes, organic halides can be formed at alkaline pH and chloride concentrations of > 1 g L^{-1} [146].

Practical, environmental and economic considerations

Besides treatment efficiency, other relevant factors may impact the choice of AOP for a specific situation. Table 2 summarizes advantages, disadvantages and potential ways to overcome certain drawbacks of discussed AOPs considering mainly practical, environmental and economic aspects.

Conclusion

Cyanobacterial blooms and toxins evidently pose a serious risk to drinking water and human health. Although cells and intracellular toxins can effectively be removed by conventional treatment, dissolved cyanotoxins require more advanced treatment such as AOPs based on reactive species including ·OH, SO_4^{-}· and other mechanisms.

However, treatment efficacy is strongly impacted by water quality parameters, where, for example, NOM, alkalinity and pH can impact reactive species stability and abundance, while pH also determines toxin speciation and susceptibility to degradation. Furthermore, NOM, chloride and bromide may function as precursors for toxic DBPs. Hence, AOPs, especially their process parameters, need to be optimized for individual situations also considering economic aspects such as operational and maintenance costs.

So far, most studies focused on single toxin removal in either pure or "simulated surface water". More research is thus needed on the degradation of environmentally relevant cyanotoxin mixtures, which are likely to co-occur in the environment, in actual surface water or water withdrawn from a drinking water treatment process prior to the oxidation step. Further, various degradation products have been tentatively identified in different studies but eventual residual toxicity of the treated cyanotoxin solution is rarely examined. Adequate toxicological assays can be recommended to ensure that toxins are not only degraded but also actually detoxified, especially if degradation products are not analyzed or if DBPs are likely to be produced during the treatment process.

It was also found that efficiency as well as estimated operational and maintenance costs of an AOP at laboratory-scale do not easily translate to full-scale treatment. Hence, there is a need for more research of pilot- and full-scale applications to promote AOPs and provide essential information to drinking water treatment plant operators. For instance, photocatalysis for water treatment has been studied for decades but there are still not many, if any at all, full-scale drinking water treatment applications.

Finally, since cyanotoxins will most likely not be the only challenge to a drinking water treatment facility, a combination of different treatment methods, including

Table 2 Advantages, disadvantages and measures to overcome drawbacks [in brackets] of different AOPs considering practical, environmental and economic aspects

AOPs	Advantages	Disadvantages
Ozonation and O_3-based AOPs	Ozonation widely employed in water treatment O_3 is more selective than ·OH and less affected by NOM O_3 decomposes to ·OH in water	Toxicity of gaseous O_3 [Needs O_3-destructor and sufficient ventilation for safe working environment[a]] O_3 production is expensive[b] Dissolved O_3 stability is affected by pH and alkalinity
Photolysis	UV often used for disinfection	Pollutant degradation requires high UV doses [UV-LEDs are mercury-free, have longer lifetime, low energy demand and operational costs[c,d]] Turbidity reduces penetration depth and attenuates light [requires removal of turbidity prior to treatment; NOM can act as photosensitizer and improve degradation]
Photolysis in combination with oxidants	UV often used for disinfection UV/H_2O_2 forms two ·OH due to homolytic cleavage H_2O_2 is easy to handle and environmentally sound Chlorine more readily activated by UV and cheaper compared to H_2O_2	Turbidity reduces penetration depth and attenuates light [requires removal of turbidity prior to treatment] Gas discharge-based UV lamps have relatively short lifetime and high energy demand [UV-LEDs are mercury-free, have longer lifetime, low energy demand and operational costs] Chlorine may yield toxic halogenated byproducts
Photocatalysis	UV often used for disinfection Most often used catalyst TiO_2 is non-toxic and cheap[e] Pollutant degradation directly by catalyst and indirectly by reactive species	Catalysts may be released into water or deposited into sludge [requires catalyst removal after treatment; heterogeneous or magnetic catalysts simplify removal; immobilized catalysts are reusable which reduces costs] TiO_2 requires UV activation [doping with other elements allows use of visible and solar light; UV-LEDs are mercury-free, have longer lifetime, low energy demand and operational costs] Turbidity reduces penetration depth and attenuates light [requires removal of turbidity prior to treatment]
Fenton oxidation	Iron is highly abundant and non-toxic, H_2O_2 is easy to handle and environmentally sound Relatively inexpensive reagents and no energy demand Can use also, e.g., ferric iron or other transition metals Potential incorporation of Fenton into iron-based coagulation by addition of H_2O_2[f,g] Photo- and sono-Fenton increase efficacy and reduce costs, especially for solar photo-Fenton	Requires acidic conditions with optimum pH ≈ 3 reported [heterogeneous or immobilized catalysts may extend pH range] Release of iron (or other transition metals) into water or deposition into sludge [requires sludge removal and its treatment; use of heterogeneous or immobilized catalyst reduces environmental release]
Non-thermal plasma	Reagent-free treatment Continuous production of reactive species, electrons and photons Degrades pollutants persistent to other AOPs[h] Residual oxidative and disinfective effect of plasma-treated water, which may reduce energy demands and costs; alternative to post-chlorination avoiding chlorine taste and odor	Residual oxidative and disinfective effect of plasma treated water may generate undesired, e.g., toxic or acidic products Requires energy input

Table 2 (continued)

AOPs	Advantages	Disadvantages
Sulfate radical-based AOPs	Various ways of PMS and PS activation, where activation by redox reactions reduces costs[i] Continuous production of reactive species in electric discharges and electrochemical processes High reactivity across broad pH spectrum SO_4^{-}· can degrade pollutants resistant to ·OH[j] Lower energy for cleavage of peroxide bond in PS SO_4^{-}· less affected by NOM and alkalinity than ·OH	Sulfate has noticeable taste at 250–500 mg L^{-1}, laxative effects at 1000–1200 mg L^{-1}, contributes to corrosion[k] Possible acidification due to dissociation of HSO_4^{-} when PMS is used[l,m]
Electrochemical oxidation	Large number of commercial electrolytes and electrodes Pollutant degradation directly at electrodes and indirectly by reactive species Continuous production of reactive species	Catalytic electrodes (Ti, Ir, Pt, BDD) have high efficiency, but are more expensive than metallic (Cu, Fe, Zn) which can produce secondary contamination[n] [Cheap and environmentally sound alternatives proposed—e.g., Ti-coated C-electrode made from pencils or carbon sticks from recycled batteries[n]] Cl-based electrolytes may lead to formation of halogenated byproducts N- and P-based electrolytes increase N and P in water (eutrophication)
Sonolysis	Reagent-free and clean technology Pollutant removal by chemical reactions, thermo- and pyrolysis, and shock-waves and shear forces Easy scale-up of hydrodynamic cavitation processes[o]	Higher energy inputs increasing the treatment costs [optimization toward lower frequencies may reduce energy demand[p]; combination with other AOPs reduces costs; hydrodynamic cavitation avoids noise, energy demand and costs] Treatment of large volumes requires greater number of ultrasound transducers[o] Cavitation is a violent process destructive to materials and requires periodical maintenance[o]
Radiolysis	Homogeneous system Use of scavengers produce specific or single reactive species valuable for studying degradation mechanisms	High capital costs and safety measures[q] Rather unsuitable for large-scale drinking water treatment

[a] [155]
[b] [13]
[c] [74]
[d] [67]
[e] [156]
[f] [97]
[g] [38]
[h] [157]
[i] [35]
[j] [118]
[k] [158]
[l] [36]
[m] [124]
[n] [128]
[o] [136]
[p] [139]
[q] [146]

different AOPs, in a multi-barrier approach needs to be considered to produce harmless, high-quality drinking water.

Abbreviations
A: Alanine; AC: Activated carbon; ANTX: Anatoxin-a; AO: Anodic oxidation; AOP: Advanced oxidation process; BDD: Boron-doped diamond; BMAA: β-*N*-methylamino-L-alanine; CYN: Cylindrospermopsin; DBP: Disinfection byproduct; EAOP: Electrochemical advanced oxidation process; E_{EO}: Electrical energy per order; EF: Electro-Fenton; GTX: Gonyautoxin; GV: Guideline value; L: Leucine; LED: Light-emitting diode; MC: Microcystin; NOD: Nodularin; NOM: Natural organic matter; NTP: Non-thermal plasma; PBS: Phosphate-buffered saline; PCB28: 2,4,4′-Trichlorobiphenyl; PEF: Photoelectro-Fenton; PET: Polyethylene terephthalate; pK_a: Negative decadic logarithm of the acid dissociation constant; PVC: Polyvinyl chloride; PMS: Peroxymonosulfate; PS: Peroxydisulfate, persulfate; R: Arginine; SHE: Standard hydrogen electrode; SR: Sulfate radical; STX: Saxitoxin; $t_{1/2}$: Half-life; TDI: Total daily intake; US EPA: United States Environmental Protection Agency; UV: Ultraviolet; Vis: Visible; WHO: World Health Organization; Y: Tyrosine.

Acknowledgements
Not applicable.

Disclaimer
Any opinions in this article only reflect the authors' views and the European Union's Research Executive Agency is not responsible for any use that may be made of the information it contains.

Authors' contributions
MS performed the literature research and drafted the manuscript; LB revised the text. Both authors read and approved the final manuscript.

Funding
This research received funding from the European Union's Horizon 2020 research and innovation program under the Marie Skłodowska-Curie Grant agreement No. 722493 NaToxAq and No. 857560 CETOCOEN EXCELLENCE Teaming 2 project. The RECETOX Research infrastructure was further supported by the Czech Ministry of Education, Youth and Sports (LM2018121; CZ0 2.1.01/0.0/0.0/18_046/0015975).

Availability of data and materials
Not applicable.

Ethics approval and consent to participate
Not applicable.

Consent for publication
Not applicable.

Competing interests
The authors declare that they have no competing interests.

Received: 19 April 2020 Accepted: 15 June 2020
Published online: 08 July 2020

References

1. Skulberg OM, Carmichael WW, Codd GA, Skulberg R (1993) Taxonomy of toxic cyanophyceae (Cyanobacteria). In: Falconer IR (ed) Algal toxins in seafood and drinking water. Academic Press, London, pp 145–164
2. Newcombe G (2009) International guidance manual for the management of toxic cyanobacteria. Global Water Research Coalition
3. Durai P, Batool M, Choi S (2015) Structure and effects of cyanobacterial lipopolysaccharides. Mar Drugs 13:4217–4230. https://doi.org/10.3390/md13074217
4. Mantzouki E, Visser PM, Bormans M, Ibelings BW (2016) Understanding the key ecological traits of cyanobacteria as a basis for their management and control in changing lakes. Aquat Ecol 50:333–350. https://doi.org/10.1007/s10452-015-9526-3
5. Codd GA, Meriluoto J, Metcalf JS (2016) Introduction. In: Meriluoto J, Spoof L, Codd GA (eds) Handbook of cyanobacterial monitoring and cyanotoxin analysis. Wiley, Hoboken, pp 1–8
6. Buratti FM, Manganelli M, Vichi S et al (2017) Cyanotoxins: producing organisms, occurrence, toxicity, mechanism of action and human health toxicological risk evaluation. Arch Toxicol 91:1049–1130. https://doi.org/10.1007/s00204-016-1913-6
7. Machado J, Campos A, Vasconcelos V, Freitas M (2017) Effects of microcystin-LR and cylindrospermopsin on plant–soil systems: a review of their relevance for agricultural plant quality and public health. Environ Res 153:191–204. https://doi.org/10.1016/j.envres.2016.09.015
8. Ibelings BW, Bormans M, Fastner J, Visser PM (2016) CYANOCOST special issue on cyanobacterial blooms: synopsis—a critical review of the management options for their prevention, control and mitigation. Aquat Ecol 50:595–605. https://doi.org/10.1007/s10452-016-9596-x
9. Westrick JA, Szlag DC, Southwell BJ, Sinclair J (2010) A review of cyanobacteria and cyanotoxins removal/inactivation in drinking water treatment. Anal Bioanal Chem 397:1705–1714. https://doi.org/10.1007/s00216-010-3709-5
10. He X, Liu Y-L, Conklin A et al (2016) Toxic cyanobacteria and drinking water: impacts, detection, and treatment. Harmful Algae 54:174–193. https://doi.org/10.1016/j.hal.2016.01.001
11. Chorus I (2005) Water safety plans. In: Huisman J, Matthijs HCP, Visser PM (eds) Harmful cyanobacteria. Springer, Dordrecht, pp 201–227
12. Ho L, Sawade E, Newcombe G (2012) Biological treatment options for cyanobacteria metabolite removal—a review. Water Res 46:1536–1548. https://doi.org/10.1016/j.watres.2011.11.018
13. Lawton LA, Robertson PKJ (1999) Physico-chemical treatment methods for the removal of microcystins (cyanobacterial hepatotoxins) from potable waters. Chem Soc Rev 28:217–224. https://doi.org/10.1039/A805416I
14. Rodríguez E, Onstad GD, Kull TPJ et al (2007) Oxidative elimination of cyanotoxins: comparison of ozone, chlorine, chlorine dioxide and permanganate. Water Res 41:3381–3393. https://doi.org/10.1016/J.WATRES.2007.03.033
15. Meriluoto J, Spoof L, Codd GA (2016) Handbook of cyanobacterial monitoring and cyanotoxin analysis. Wiley, Chichester
16. Catherine A, Bernard C, Spoof L, Bruno M (2016) Microcystins and nodularins. In: Meriluoto J, Spoof L, Codd GA (eds) Handbook of cyanobacterial monitoring and cyanotoxin analysis. Wiley, Chichester, pp 107–126
17. Ministry of Health (2017) Guidelines for drinking-water quality management for New Zealand, 3rd edn. Ministry of Health, Wellington
18. Kokociński M, Cameán AM, Carmeli S et al (2016) Cylindrospermopsin and congeners. In: Meriluoto J, Spoof L, Codd GA (eds) Handbook of cyanobacterial monitoring and cyanotoxin analysis. Wiley, Hoboken, pp 127–137
19. Onstad GD, Strauch S, Meriluoto J et al (2007) Selective oxidation of key functional groups in cyanotoxins during drinking water ozonation. Environ Sci Technol 41:4397–4404. https://doi.org/10.1021/es0625327
20. Bruno M, Ploux O, Metcalf JS et al (2016) Anatoxin-a, Homoanatoxin-a, and natural analogues. In: Meriluoto J, Spoof L, Codd GA (eds) Handbook of cyanobacterial monitoring and cyanotoxin analysis. Wiley, Hoboken, pp 138–147
21. Ballot A, Bernard C, Fastner J (2016) Saxitoxin and analogues. In: Meriluoto J, Spoof L, Codd GA (eds) Handbook of cyanobacterial monitoring and cyanotoxin analysis. Wiley, Hoboken, pp 148–154
22. Ploux O, Combes A, Eriksson J, Metcalf JS (2016) β-*N*-Methylamino-L-alanine and (S)-2,4-diaminobutyric acid. In: Meriluoto J, Spoof L, Codd GA (eds) Handbook of cyanobacterial monitoring and cyanotoxin analysis. Wiley, Hoboken, pp 160–164
23. Carmichael WW (1992) Cyanobacteria secondary metabolites—the cyanotoxins. J Appl Bacteriol 72:445–459. https://doi.org/10.1111/j.1365-2672.1992.tb01858.x
24. Griffiths DJ, Saker ML (2003) The Palm Island mystery disease 20 years on: a review of research on the cyanotoxin cylindrospermopsin. Environ Toxicol 18:78–93. https://doi.org/10.1002/tox.10103
25. Carmichael WW, Azevedo SM, An JS et al (2001) Human fatalities from cyanobacteria: chemical and biological evidence for cyanotoxins. Environ Health Perspect 109:663–668

26. Brooks BW, Lazorchak JM, Howard MDA et al (2016) Are harmful algal blooms becoming the greatest inland water quality threat to public health and aquatic ecosystems? Environ Toxicol Chem 35:6–13. https://doi.org/10.1002/etc.3220
27. Svirčev Z, Drobac D, Tokodi N et al (2016) Lessons from the Užice case. In: Meriluoto J, Spoof L, Codd GA (eds) Handbook of cyanobacterial monitoring and cyanotoxin analysis. Wiley, Hoboken, pp 298–308
28. Fitzsimmons EG (2014) Tap water ban for toledo residents. New York Times
29. Wilson E (2014) Danger from microcystins in toledo water unclear. Chem Eng News 92:9
30. WHO (2003) Cyanobacterial toxins: microcystin-LR in drinking-water. Background document for preparation of WHO guidelines for drinking-water quality. World Health Organization, Geneva
31. Drinking-water quality guidelines. https://www.who.int/water_sanitation_health/water-quality/guidelines/en/. Accessed 27 Mar 2020
32. Chorus I (2012) Current approaches to Cyanotoxin risk assessment, risk management and regulations in different countries. Federal Environment Agency, Dessau-Roßlau
33. Schwarzenbach RP, Gschwend PM, Imboden DM (2002) Indirect photolysis: reactions with photooxidants in natural waters and in the atmosphere. Environmental organic chemistry. Wiley, Hoboken, pp 655–686
34. von Sonntag C, von Gunten U (2012) Reactions of hydroxyl and peroxyl radicals. Chemistry of ozone in water and wastewater treatment: from basic principles to applications. IWA Publishing, London, pp 225–248
35. Zhang B-T, Zhang Y, Teng Y, Fan M (2015) Sulfate radical and its application in decontamination technologies. Crit Rev Environ Sci Technol 45:1756–1800. https://doi.org/10.1080/10643389.2014.970681
36. Antoniou MG, de la Cruz AA, Dionysiou DD (2010) Degradation of microcystin-LR using sulfate radicals generated through photolysis, thermolysis and e-transfer mechanisms. Appl Catal B Environ 96:290–298. https://doi.org/10.1016/J.APCATB.2010.02.013
37. Chen Y-T, Chen W-R, Lin T-F (2018) Oxidation of cyanobacterial neurotoxin beta-*N*-methylamino-L-alanine (BMAA) with chlorine, permanganate, ozone, hydrogen peroxide and hydroxyl radical. Water Res 142:187–195. https://doi.org/10.1016/J.WATRES.2018.05.056
38. Park J-A, Yang B, Park C et al (2017) Oxidation of microcystin-LR by the Fenton process: kinetics, degradation intermediates, water quality and toxicity assessment. Chem Eng J 309:339–348. https://doi.org/10.1016/j.cej.2016.10.083
39. Tak S-Y, Kim M-K, Lee J-E et al (2018) Degradation mechanism of anatoxin-a in UV-C/H_2O_2 reaction. Chem Eng J 334:1016–1022. https://doi.org/10.1016/J.CEJ.2017.10.081
40. He X, de la Cruz AA, Dionysiou DD (2013) Destruction of cyanobacterial toxin cylindrospermopsin by hydroxyl radicals and sulfate radicals using UV-254 nm activation of hydrogen peroxide, persulfate and peroxymonosulfate. J Photochem Photobiol A Chem 251:160–166. https://doi.org/10.1016/J.JPHOTOCHEM.2012.09.017
41. He X, de la Cruz AA, Hiskia A et al (2015) Destruction of microcystins (cyanotoxins) by UV-254 nm-based direct photolysis and advanced oxidation processes (AOPs): influence of variable amino acids on the degradation kinetics and reaction mechanisms. Water Res 74:227–238. https://doi.org/10.1016/J.WATRES.2015.02.011
42. von Sonntag C, von Gunten U (2012) Chemistry of ozone in water and wastewater treatment: from basic principles to applications. IWA Publishing, London
43. Von Gunten U (2003) Ozonation of drinking water: part I. Oxidation kinetics and product formation. Water Res 37:1443–1467. https://doi.org/10.1016/S0043-1354(02)00457-8
44. Al Momani F (2007) Degradation of cyanobacteria anatoxin-a by advanced oxidation processes. Sep Purif Technol 57:85–93. https://doi.org/10.1016/J.SEPPUR.2007.03.008
45. Al Momani F, Smith DW, Gamal El-Din M (2008) Degradation of cyanobacteria toxin by advanced oxidation processes. J Hazard Mater 150:238–249. https://doi.org/10.1016/j.jhazmat.2007.04.087
46. Yan S, Jia A, Merel S et al (2016) Ozonation of cylindrospermopsin (cyanotoxin): degradation mechanisms and cytotoxicity assessments. Environ Sci Technol 50:1437–1446. https://doi.org/10.1021/acs.est.5b04540
47. Orr PT, Jones GJ, Hamilton GR (2004) Removal of saxitoxins from drinking water by granular activated carbon, ozone and hydrogen peroxide—implications for compliance with the Australian drinking water guidelines. Water Res 38:4455–4461. https://doi.org/10.1016/J.WATRES.2004.08.024
48. Bober B, Pudas K, Lechowski Z, Bialczyk J (2008) Degradation of microcystin-LR by ozone in the presence of Fenton reagent. J Environ Sci Health A Tox Hazard Subst Environ Eng 43:186–190. https://doi.org/10.1080/10934520701781582
49. Wu C-C, Huang W-J, Ji B-H (2015) Degradation of cyanotoxin cylindrospermopsin by TiO_2-assisted ozonation in water. J Environ Sci Health A Tox Hazard Subst Environ Eng 50:1116–1126. https://doi.org/10.1080/10934529.2015.1047664
50. Schwarzenbach RP, Gschwend PM, Imboden DM (2002) Direct photolysis. Environmental organic chemistry. Wiley, Hoboken, pp 611–654
51. Stevens DK, Krieger RI (1991) Stability studies on the cyanobacterial nicotinic alkaloid anatoxin-A. Toxicon 29:167–179. https://doi.org/10.1016/0041-0101(91)90101-V
52. Wörmer L, Huerta-Fontela M, Cirés S et al (2010) Natural photodegradation of the cyanobacterial toxins microcystin and cylindrospermopsin. Environ Sci Technol 44:3002–3007. https://doi.org/10.1021/es9036012
53. Mazur-Marzec H, Meriluoto J, Pliński M (2006) The degradation of the cyanobacterial hepatotoxin nodularin (NOD) by UV radiation. Chemosphere 65:1388–1395. https://doi.org/10.1016/J.CHEMOSPHERE.2006.03.072
54. Afzal A, Oppenländer T, Bolton JR, El-Din MG (2010) Anatoxin-a degradation by advanced oxidation processes: vacuum-UV at 172 nm, photolysis using medium pressure UV and UV/H_2O_2. Water Res 44:278–286. https://doi.org/10.1016/J.WATRES.2009.09.021
55. Moon B-R, Kim T-K, Kim M-K et al (2017) Degradation mechanisms of Microcystin-LR during UV-B photolysis and UV/H_2O_2 processes: byproducts and pathways. Chemosphere 185:1039–1047. https://doi.org/10.1016/J.CHEMOSPHERE.2017.07.104
56. Chang J, Chen Z, Wang Z et al (2015) Oxidation of microcystin-LR in water by ozone combined with UV radiation: the removal and degradation pathway. Chem Eng J 276:97–105. https://doi.org/10.1016/J.CEJ.2015.04.070
57. Liu Y, Ren J, Wang X, Fan Z (2016) Mechanism and reaction pathways for microcystin-LR degradation through UV/H_2O_2 treatment. PLoS ONE 11:e0156236
58. Tsuji K, Naito S, Kondo F et al (1994) Stability of microcystins from cyanobacteria: effect of light on decomposition and isomerization. Environ Sci Technol 28:173–177. https://doi.org/10.1021/es00050a024
59. Gajdek P, Bober B, Mej E, Bialczyk J (2004) Sensitised decomposition of microcystin-LR using UV radiation. J Photochem Photobiol B Biol 76:103–106. https://doi.org/10.1016/J.JPHOTOBIOL.2004.06.001
60. Verma S, Sillanpää M (2015) Degradation of anatoxin-a by UV-C LED and UV-C LED/H_2O_2 advanced oxidation processes. Chem Eng J 274:274–281. https://doi.org/10.1016/J.CEJ.2015.03.128
61. Song W, Yan S, Cooper WJ et al (2012) Hydroxyl radical oxidation of cylindrospermopsin (cyanobacterial toxin) and its role in the photochemical transformation. Environ Sci Technol 46:12608–12615. https://doi.org/10.1021/es302458h
62. Chiswell RK, Shaw GR, Eaglesham G et al (1999) Stability of cylindrospermopsin, the toxin from the cyanobacterium, *Cylindrospermopsis raciborskii*: effect of pH, temperature, and sunlight on decomposition. Environ Toxicol 14:155–161. https://doi.org/10.1002/(SICI)1522-7278(199902)14:1%3c155:AID-TOX20%3e3.0.CO;2-Z
63. Adamski M, Żmudzki P, Chrapusta E et al (2016) Characterization of cylindrospermopsin decomposition products formed under irradiation conditions. Algal Res 18:1–6. https://doi.org/10.1016/J.ALGAL.2016.05.027
64. Zhang X, He J, Xiao S, Yang X (2019) Elimination kinetics and detoxification mechanisms of microcystin-LR during UV/chlorine process. Chemosphere 214:702–709. https://doi.org/10.1016/J.CHEMOSPHERE.2018.09.162
65. Park J-A, Yang B, Jang M et al (2019) Oxidation and molecular properties of microcystin-LR, microcystin-RR and anatoxin-a using UV-light-emitting diodes at 255 nm in combination with H_2O_2. Chem Eng J 366:423–432. https://doi.org/10.1016/J.CEJ.2019.02.101

66. Liu X, Chen Z, Zhou N et al (2010) Degradation and detoxification of microcystin-LR in drinking water by sequential use of UV and ozone. J Environ Sci 22:1897–1902. https://doi.org/10.1016/S1001-0742(09)60336-3
67. Duan X, Sanan T, de la Cruz A et al (2018) Susceptibility of the algal toxin microcystin-LR to UV/chlorine process: comparison with chlorination. Environ Sci Technol 52:8252–8262. https://doi.org/10.1021/acs.est.8b00034
68. Park J-A, Yang B, Kim J-H et al (2018) Removal of microcystin-LR using UV-assisted advanced oxidation processes and optimization of photo-Fenton-like process for treating Nak-Dong River water, South Korea. Chem Eng J 348:125–134. https://doi.org/10.1016/J.CEJ.2018.04.190
69. He X, Zhang G, de la Cruz AA et al (2014) Degradation mechanism of cyanobacterial toxin cylindrospermopsin by hydroxyl radicals in homogeneous UV/H_2O_2 process. Environ Sci Technol 48:4495–4504. https://doi.org/10.1021/es403732s
70. Ochando-Pulido JM, Hodaifa G, Víctor-Ortega MD, Martínez-Ferez A (2013) A novel photocatalyst with ferromagnetic core used for the treatment of olive oil mill effluents from two-phase production process. ScientificWorldJournal 2013:196470. https://doi.org/10.1155/2013/196470
71. Fotiou T, Triantis TM, Kaloudis T et al (2016) Assessment of the roles of reactive oxygen species in the UV and visible light photocatalytic degradation of cyanotoxins and water taste and odor compounds using C-TiO_2. Water Res 90:52–61. https://doi.org/10.1016/J.WATRES.2015.12.006
72. Chen L, Zhao C, Dionysiou DD, O'Shea KE (2015) TiO_2 photocatalytic degradation and detoxification of cylindrospermopsin. J Photochem Photobiol A Chem 307–308:115–122. https://doi.org/10.1016/J.JPHOTOCHEM.2015.03.013
73. Triantis TM, Fotiou T, Kaloudis T et al (2012) Photocatalytic degradation and mineralization of microcystin-LR under UV-A, solar and visible light using nanostructured nitrogen doped TiO_2. J Hazard Mater 211–212:196–202. https://doi.org/10.1016/J.JHAZMAT.2011.11.042
74. Pestana CJ, Edwards C, Prabhu R et al (2015) Photocatalytic degradation of eleven microcystin variants and nodularin by TiO_2 coated glass microspheres. J Hazard Mater 300:347–353. https://doi.org/10.1016/J.JHAZMAT.2015.07.016
75. Lawton LA, Robertson PKJ, Cornish BJPA et al (2003) Processes influencing surface interaction and photocatalytic destruction of microcystins on titanium dioxide photocatalysts. J Catal 213:109–113. https://doi.org/10.1016/S0021-9517(02)00049-0
76. Pelaez M, de la Cruz AA, O'Shea K et al (2011) Effects of water parameters on the degradation of microcystin-LR under visible light-activated TiO2 photocatalyst. Water Res 45:3787–3796. https://doi.org/10.1016/J.WATRES.2011.04.036
77. Pelaez M, de la Cruz AA, Stathatos E et al (2009) Visible light-activated N-F-codoped TiO_2 nanoparticles for the photocatalytic degradation of microcystin-LR in water. Catal Today 144:19–25. https://doi.org/10.1016/J.CATTOD.2008.12.022
78. Zhao C, Pelaez M, Dionysiou DD et al (2014) UV and visible light activated TiO_2 photocatalysis of 6-hydroxymethyl uracil, a model compound for the potent cyanotoxin cylindrospermopsin. Catal Today 224:70–76. https://doi.org/10.1016/J.CATTOD.2013.09.042
79. Han C, Pelaez M, Likodimos V et al (2011) Innovative visible light-activated sulfur doped TiO_2 films for water treatment. Appl Catal B Environ 107:77–87. https://doi.org/10.1016/J.APCATB.2011.06.039
80. Pelaez M, Falaras P, Likodimos V et al (2016) Use of selected scavengers for the determination of NF-TiO_2 reactive oxygen species during the degradation of microcystin-LR under visible light irradiation. J Mol Catal A Chem 425:183–189. https://doi.org/10.1016/J.MOLCATA.2016.09.035
81. Zhao C, Li D, Liu Y et al (2015) Photocatalytic removal of microcystin-LR by advanced WO3-based nanoparticles under simulated solar light. ScientificWorldJournal 2015:720706. https://doi.org/10.1155/2015/720706
82. Han C, Machala L, Medrik I et al (2017) Degradation of the cyanotoxin microcystin-LR using iron-based photocatalysts under visible light illumination. Environ Sci Pollut Res 24:19435–19443. https://doi.org/10.1007/s11356-017-9566-4
83. Wang S, Ma W, Fang Y et al (2014) Bismuth oxybromide promoted detoxification of cylindrospermopsin under UV and visible light illumination. Appl Catal B Environ 150–151:380–388. https://doi.org/10.1016/J.APCATB.2013.12.016
84. Yanfen F, Yingping H, Jing Y et al (2011) Unique ability of BiOBr to decarboxylate d-Glu and d-MeAsp in the photocatalytic degradation of microcystin-LR in water. Environ Sci Technol 45:1593–1600. https://doi.org/10.1021/es103422j
85. Pinho LX, Azevedo J, Miranda SM et al (2015) Oxidation of microcystin-LR and cylindrospermopsin by heterogeneous photocatalysis using a tubular photoreactor packed with different TiO_2 coated supports. Chem Eng J 266:100–111. https://doi.org/10.1016/J.CEJ.2014.12.023
86. Lee D-K, Kim S-C, Kim S-J et al (2004) Photocatalytic oxidation of microcystin-LR with TiO_2-coated activated carbon. Chem Eng J 102:93–98. https://doi.org/10.1016/J.CEJ.2004.01.027
87. Cornish BJP, Lawton LA, Robertson PK (2000) Hydrogen peroxide enhanced photocatalytic oxidation of microcystin-LR using titanium dioxide. Appl Catal B Environ 25:59–67. https://doi.org/10.1016/S0926-3373(99)00121-6
88. Bessegato GG, Guaraldo TT, de Brito JF et al (2015) Achievements and trends in photoelectrocatalysis: from environmental to energy applications. Electrocatalysis 6:415–441. https://doi.org/10.1007/s12678-015-0259-9
89. Liao W, Zhang Y, Zhang M et al (2013) Photoelectrocatalytic degradation of microcystin-LR using Ag/AgCl/TiO_2 nanotube arrays electrode under visible light irradiation. Chem Eng J 231:455–463. https://doi.org/10.1016/J.CEJ.2013.07.054
90. Moreira FC, Boaventura RAR, Brillas E, Vilar VJP (2017) Electrochemical advanced oxidation processes: a review on their application to synthetic and real wastewaters. Appl Catal B Environ 202:217–261. https://doi.org/10.1016/j.apcatb.2016.08.037
91. Liu J, Hernández SE, Swift S, Singhal N (2018) Estrogenic activity of cylindrospermopsin and anatoxin-a and their oxidative products by FeIII-B*/H2O2. Water Res 132:309–319. https://doi.org/10.1016/J.WATRES.2018.01.018
92. Munoz M, Nieto-Sandoval J, Cirés S et al (2019) Degradation of widespread cyanotoxins with high impact in drinking water (microcystins, cylindrospermopsin, anatoxin-a and saxitoxin) by CWPO. Water Res 163:114853. https://doi.org/10.1016/J.WATRES.2019.114853
93. Zhong Y, Jin X, Qiao R et al (2009) Destruction of microcystin-RR by Fenton oxidation. J Hazard Mater 167:1114–1118. https://doi.org/10.1016/J.JHAZMAT.2009.01.117
94. Jung YS, Lim WT, Park J, Kim Y (2009) Effect of pH on fenton and fenton-like oxidation. Environ Technol 30:183–190. https://doi.org/10.1080/09593330802468848
95. Fang Y-F, Chen D-X, Huang Y-P et al (2011) Heterogeneous fenton photodegradation of microcystin-LR with visible light irradiation. Chinese J Anal Chem 39:540–543. https://doi.org/10.1016/S1872-2040(10)60433-1
96. Lee H, Lee H-J, Sedlak DL, Lee C (2013) pH-Dependent reactivity of oxidants formed by iron and copper-catalyzed decomposition of hydrogen peroxide. Chemosphere 92:652–658. https://doi.org/10.1016/J.CHEMOSPHERE.2013.01.073
97. Gajdek P, Lechowski Z, Bochnia T, Kępczyński M (2001) Decomposition of microcystin-LR by Fenton oxidation. Toxicon 39:1575–1578. https://doi.org/10.1016/S0041-0101(01)00139-8
98. Zhou S, Yu Y, Sun J et al (2018) Oxidation of microcystin-LR by copper (II) coupled with ascorbic acid: kinetic modeling towards generation of H_2O_2. Chem Eng J 333:443–450. https://doi.org/10.1016/J.CEJ.2017.09.166
99. Bandala ER, Martínez D, Martínez E, Dionysiou DD (2004) Degradation of microcystin-LR toxin by Fenton and Photo-Fenton processes. Toxicon 43:829–832. https://doi.org/10.1016/j.toxicon.2004.03.013
100. de Freitas AM, Sirtori C, Lenz CA, Peralta Zamora PG (2013) Microcystin-LR degradation by solar photo-Fenton, UV-A/photo-Fenton and UV-C/H_2O_2: a comparative study. Photochem Photobiol Sci 12:696–702. https://doi.org/10.1039/C2PP25233C
101. Ma Y-S (2012) Short review: current trends and future challenges in the application of sono-Fenton oxidation for wastewater treatment. Sustain Environ Res 22:271–278
102. Karci A, Wurtzler EM, de la Cruz AA et al (2018) Solar photo-Fenton treatment of microcystin-LR in aqueous environment: transformation

products and toxicity in different water matrices. J Hazard Mater 349:282–292. https://doi.org/10.1016/J.JHAZMAT.2017.12.071
103. Wang F, Wu Y, Gao Y et al (2016) Effect of humic acid, oxalate and phosphate on Fenton-like oxidation of microcystin-LR by nanoscale zero-valent iron. Sep Purif Technol 170:337–343. https://doi.org/10.1016/J.SEPPUR.2016.06.046
104. Scholtz V, Pazlarova J, Souskova H et al (2015) Nonthermal plasma—a tool for decontamination and disinfection. Biotechnol Adv 33:1108–1119. https://doi.org/10.1016/J.BIOTECHADV.2015.01.002
105. Meichsner J, Schmidt M, Schneider R, Wagner HE (2013) Introduction. Nonthermal plasma chemistry and physics. CRC Press, Boca Raton, pp 1–6
106. Meichsner J, Schmidt M, Schneider R, Wagner HE (2013) Selected applications. Nonthermal plasma chemistry and physics. CRC Press, Boca Raton, pp 285–406
107. Banaschik R, Lukes P, Miron C et al (2017) Fenton chemistry promoted by sub-microsecond pulsed corona plasmas for organic micropollutant degradation in water. Electrochim Acta 245:539–548. https://doi.org/10.1016/J.ELECTACTA.2017.05.121
108. Jo J-O, Jwa E, Mok Y-S (2016) Decomposition of aqueous anatoxin-a using underwater dielectric barrier discharge plasma created in a porous ceramic tube. J Korean Soc Water Wastewater 30:167–177. https://doi.org/10.11001/jksww.2016.30.2.167
109. Zhang H, Huang Q, Ke Z et al (2012) Degradation of microcystin-LR in water by glow discharge plasma oxidation at the gas-solution interface and its safety evaluation. Water Res 46:6554–6562. https://doi.org/10.1016/j.watres.2012.09.041
110. Banaschik R, Jablonowski H, Bednarski PJ, Kolb JF (2018) Degradation and intermediates of diclofenac as instructive example for decomposition of recalcitrant pharmaceuticals by hydroxyl radicals generated with pulsed corona plasma in water. J Hazard Mater 342:651–660. https://doi.org/10.1016/J.JHAZMAT.2017.08.058
111. Xin Q, Zhang Y, Wu K (2013) Degradation of microcystin-LR by gas–liquid interfacial discharge plasma. Plasma Sci Technol 15:1221
112. Xin Q, Zhang Y, Wu KB (2013) Mn-doped carbon xerogels as catalyst in the removal of microcystin-LR by water-surface discharge plasma. J Environ Sci Health A Toxic Hazard Subst Environ Eng 48:293–299. https://doi.org/10.1080/10934529.2013.726833
113. Nisol B, Watson S, Leblanc Y et al (2019) Cold plasma oxidation of harmful algae and associated metabolite BMAA toxin in aqueous suspension. Plasma Process Polym 16:1800137. https://doi.org/10.1002/ppap.201800137
114. Xin Q, Zhang Y, Li Z et al (2015) Mn/Ti-doped carbon xerogel for efficient catalysis of microcystin-LR degradation in the water surface discharge plasma reactor. Environ Sci Pollut Res 22:17202–17208. https://doi.org/10.1007/s11356-015-4956-y
115. Zhang Y, Wei H, Xin Q et al (2016) Process optimization for microcystin-LR degradation by response surface methodology and mechanism analysis in gas–liquid hybrid discharge system. J Environ Manage 183:726–732. https://doi.org/10.1016/j.jenvman.2016.09.030
116. Pekárek S (2012) Experimental study of surface dielectric barrier discharge in air and its ozone production. J Phys D Appl Phys 45:75201. https://doi.org/10.1088/0022-3727/45/7/075201
117. Matzek LW, Carter KE (2016) Activated persulfate for organic chemical degradation: a review. Chemosphere 151:178–188. https://doi.org/10.1016/J.CHEMOSPHERE.2016.02.055
118. Wacławek S, Lutze HV, Grübel K et al (2017) Chemistry of persulfates in water and wastewater treatment: a review. Chem Eng J 330:44–62. https://doi.org/10.1016/J.CEJ.2017.07.132
119. Son G, Lee H (2016) Methylene blue removal by submerged plasma irradiation system in the presence of persulfate. Environ Sci Pollut Res 23:15651–15656. https://doi.org/10.1007/s11356-016-6759-1
120. Bakheet B, Islam MA, Beardall J et al (2018) Electrochemical inactivation of *Cylindrospermopsis raciborskii* and removal of the cyanotoxin cylindrospermopsin. J Hazard Mater 344:241–248. https://doi.org/10.1016/J.JHAZMAT.2017.10.024
121. Yang Y, Jiang J, Lu X et al (2015) Production of sulfate radical and hydroxyl radical by reaction of ozone with peroxymonosulfate: a novel advanced oxidation process. Environ Sci Technol 49:7330–7339. https://doi.org/10.1021/es506362e
122. Lou X, Wu L, Guo Y et al (2014) Peroxymonosulfate activation by phosphate anion for organics degradation in water. Chemosphere 117:582–585. https://doi.org/10.1016/J.CHEMOSPHERE.2014.09.046
123. Antoniou MG, de la Cruz AA, Dionysiou DD (2010) Intermediates and reaction pathways from the degradation of microcystin-LR with sulfate radicals. Environ Sci Technol 44:7238–7244. https://doi.org/10.1021/es1000243
124. Verma S, Nakamura S, Sillanpää M (2016) Application of UV-C LED activated PMS for the degradation of anatoxin-a. Chem Eng J 284:122–129. https://doi.org/10.1016/J.CEJ.2015.08.095
125. He X, de la Cruz AA, O'Shea KE, Dionysiou DD (2014) Kinetics and mechanisms of cylindrospermopsin destruction by sulfate radical-based advanced oxidation processes. Water Res 63:168–178. https://doi.org/10.1016/J.WATRES.2014.06.004
126. Antoniou MG, Boraei I, Solakidou M et al (2018) Enhancing photocatalytic degradation of the cyanotoxin microcystin-LR with the addition of sulfate-radical generating oxidants. J Hazard Mater 360:461–470. https://doi.org/10.1016/J.JHAZMAT.2018.07.111
127. Fang G, Gao J, Dionysiou DD et al (2013) Activation of persulfate by quinones: free radical reactions and implication for the degradation of PCBs. Environ Sci Technol 47:4605–4611. https://doi.org/10.1021/es400262n
128. Sanz Lobón G, Yepez A, Garcia LF et al (2017) Efficient electrochemical remediation of microcystin-LR in tap water using designer TiO(2)@carbon electrodes. Sci Rep 7:41326. https://doi.org/10.1038/srep41326
129. Tran N, Drogui P (2013) Electrochemical removal of microcystin-LR from aqueous solution in the presence of natural organic pollutants. J Environ Manage 114:253–260. https://doi.org/10.1016/J.JENVMAN.2012.10.009
130. Zhou S, Bu L, Yu Y et al (2016) A comparative study of microcystin-LR degradation by electrogenerated oxidants at BDD and MMO anodes. Chemosphere 165:381–387. https://doi.org/10.1016/J.CHEMOSPHERE.2016.09.057
131. Santos PVF, Lopes IC, Diculescu VC et al (2011) Redox mechanisms of nodularin and chemically degraded nodularin. Electroanalysis 23:2310–2319. https://doi.org/10.1002/elan.201100246
132. Liang W, Qu J, Wang K et al (2008) Electrochemical degradation of cyanobacterial toxin microcystin-LR using Ti/RuO_2 electrodes in a continuous tubular reactor. Environ Eng Sci 25:635–642. https://doi.org/10.1089/ees.2006.0273
133. Zhang C, Fu D, Gu Z (2009) Degradation of microcystin-RR using boron-doped diamond electrode. J Hazard Mater 172:847–853. https://doi.org/10.1016/J.JHAZMAT.2009.07.071
134. Zhou S, Bu L, Shi Z et al (2018) Electrochemical inactivation of *Microcystis aeruginosa* using BDD electrodes: kinetic modeling of microcystins release and degradation. J Hazard Mater 346:73–81. https://doi.org/10.1016/J.JHAZMAT.2017.12.023
135. Zhang Y, Zhang Y, Yang N et al (2013) Electrochemical degradation and mechanistic analysis of microcystin-LR. J Chem Technol Biotechnol 88:1529–1537. https://doi.org/10.1002/jctb.3999
136. Gągol M, Przyjazny A, Boczkaj G (2018) Wastewater treatment by means of advanced oxidation processes based on cavitation—a review. Chem Eng J 338:599–627. https://doi.org/10.1016/J.CEJ.2018.01.049
137. Song W, de la Cruz AA, Rein K, O'Shea KE (2006) Ultrasonically induced degradation of microcystin-LR and -RR: identification of products, effect of pH, formation and destruction of peroxides. Environ Sci Technol 40:3941–3946. https://doi.org/10.1021/es0521730
138. Song W, Teshiba T, Rein K, O'Shea KE (2005) Ultrasonically induced degradation and detoxification of microcystin-LR (cyanobacterial toxin). Environ Sci Technol 39:6300–6305. https://doi.org/10.1021/es048350z
139. Shi J, Han X, Zhu Z, Deng H (2012) Identification of cytotoxicity intermediate products and degradation pathways for microcystins using low-frequency ultrasonic irradiation. Water Air Soil Pollut 223:5027–5038. https://doi.org/10.1007/s11270-012-1254-x
140. Ma B, Chen Y, Hao H et al (2005) Influence of ultrasonic field on microcystins produced by bloom-forming algae. Colloids Surf B Biointerfaces 41:197–201. https://doi.org/10.1016/J.COLSURFB.2004.12.010
141. Choppin G, Liljenzin J-O, Rydberg J, Ekberg C (2013) Absorption of nuclear radiation. Radiochemistry and nuclear chemistry. Elsevier, Amsterdam, pp 163–208

142. Choppin G, Liljenzin J-O, Rydberg J, Ekberg C (2013) Radiation effects on matter. Radiochemistry and nuclear chemistry. Elsevier, Amsterdam, pp 209–237
143. Song W, Xu T, Cooper WJ et al (2009) Radiolysis studies on the destruction of microcystin-LR in aqueous solution by hydroxyl radicals. Environ Sci Technol 43:1487–1492. https://doi.org/10.1021/es802282n
144. Zhang JB, Zheng Z, Yang GJ, Zhao YF (2007) Degradation of microcystin by gamma irradiation. Nucl Instruments Methods Phys Res Sect A Accel Spectrom Detect Assoc Equip 580:687–689. https://doi.org/10.1016/J.NIMA.2007.05.109
145. Liu S, Zhao Y, Ma F et al (2015) Control of Microcystis aeruginosa growth and associated microcystin cyanotoxin remediation by electron beam irradiation (EBI). RSC Adv 5:31292–31297. https://doi.org/10.1039/C5RA00430F
146. Miklos DB, Remy C, Jekel M et al (2018) Evaluation of advanced oxidation processes for water and wastewater treatment—a critical review. Water Res 139:118–131. https://doi.org/10.1016/J.WATRES.2018.03.042
147. Rosenfeldt EJ, Linden KG, Canonica S, von Gunten U (2006) Comparison of the efficiency of OH radical formation during ozonation and the advanced oxidation processes O3/H_2O_2 and UV/H_2O_2. Water Res 40:3695–3704. https://doi.org/10.1016/J.WATRES.2006.09.008
148. Liu J, Ye J-S, Ou H-S, Lin J (2017) Effectiveness and intermediates of microcystin-LR degradation by UV/H2O2 via 265 nm ultraviolet light-emitting diodes. Environ Sci Pollut Res Int 24:4676–4684. https://doi.org/10.1007/s11356-016-8148-1
149. Schneider O, Liang R, Bragg L et al (2019) Photocatalytic degradation of microcystins by TiO_2 using UV-LED controlled periodic illumination. Catalysts 9:181. https://doi.org/10.3390/catal9020181
150. WHO (2005) Bromate in drinking-water. Background document for development of WHO guidelines for drinking-water quality. World Health Organization, Geneva
151. WHO (2005) Trihalomethanes in drinking-water. Background document for development of WHO guidelines for drinking-water quality. World Health Organization, Geneva
152. WHO (2016) Perchlorate in drinking-water. Background document for development of WHO guidelines for drinking-water quality. World Health Organization, Geneva
153. von Gunten U, Hoigne J (1994) Bromate formation during ozonization of bromide-containing waters: interaction of ozone and hydroxyl radical reactions. Environ Sci Technol 28:1234–1242. https://doi.org/10.1021/es00056a009
154. Lutze H (2013) Sulfate radical based oxidation in water treatment (Doctoral Dissertation). University of Duisburg-Essen, Department of Instrumental Analytical Chemistry
155. Rakness KL (2005) Introduction. In: Rakness KL (ed) Ozone in drinking water treatment: process design, operation, and optimization, 1st edn. American Water Works Association, Denver, pp 1–16
156. Lawton LA, Robertson PKJ, Cornish BJPA, Jaspars M (1999) Detoxification of microcystins (cyanobacterial hepatotoxins) using TiO_2 photocatalytic oxidation. Environ Sci Technol 33:771–775. https://doi.org/10.1021/es9806682
157. Banaschik R, Lukes P, Jablonowski H et al (2015) Potential of pulsed corona discharges generated in water for the degradation of persistent pharmaceutical residues. Water Res 84:127–135. https://doi.org/10.1016/J.WATRES.2015.07.018
158. WHO (2004) Sulfate in drinking-water. Background document for development of WHO guidelines for drinking-water quality. World Health Organization, Geneva

Publisher's Note

Springer Nature remains neutral with regard to jurisdictional claims in published maps and institutional affiliations.

Submit your manuscript to a SpringerOpen journal and benefit from:

- ► Convenient online submission
- ► Rigorous peer review
- ► Open access: articles freely available online
- ► High visibility within the field
- ► Retaining the copyright to your article

Submit your next manuscript at ► springeropen.com